Energy & Buildings 298 (2023) 113481

Contents lists available at ScienceDirect

Energy & Buildings

journal homepage: www.elsevier.com/locate/enbuild

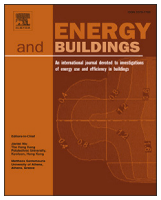

An evaluation of the demand response potential of integrated dynamic window and HVAC systems

Christoph Gehbauer *, Eleanor S. Lee, Taoning Wang

Lawrence Berkeley National Laboratory, Berkeley, CA, United States of America

ARTICLE INFO

Keywords:
Demand response
Resource adequacy
Model predictive control
Switchable windows
Dynamic facades
Building energy efficiency
Daylighting

ABSTRACT

Demand response (DR) increases the flexibility and reliability of the electricity grid as use of intermittent renewable energy sources increases. HVAC and envelope DR measures present the largest aggregate energy and peak demand savings potential of all commercial building end uses because their net demand savings occur during critical peak demand periods. Controllable envelope measures include switchable electrochromic windows, operable window attachments such as outdoor louvers, roller shades, and awnings, as well as other innovative facade technologies that can modulate both solar heat gain and daylight admission over a broad solar-optical range. This study evaluated the technical potential of DR-enabled dynamic windows to reduce critical peak demand for a prototypical medium office building situated in all 16 U.S. climates. Model predictive control (MPC) algorithms were designed to minimize electricity cost in daylit perimeter office zones through control of an electrochromic window with and without HVAC thermostat setpoint control. Conventional and time-of-use rates were used to shape the degree of DR. Median annual peak demand savings with window and thermostat control across all climate zones were 24.3 kW (4.4 W/m^2) per building or 15.9 W/m^2 for non-north perimeter zones. Resource adequacy at the whole building level was estimated to be 13.1 to 43.4 $/kW per year over the 30-year life of the installation. Co-benefits were increased energy efficiency, and reduced electricity cost and emissions. Visual and thermal comfort requirements were met at all times. Dynamic facades controlled by MPC have substantial technical potential for DR across all U.S. climates and warrant serious consideration for inclusion in DR portfolios.

1. Introduction

With increased adoption of renewable distributed energy resources (DER), there is an urgent need to develop and deploy demand response (DR) measures to increase flexibility and reliability of the electricity grid [1]. Unlike conventional generation, clean renewable sources based on solar and wind provide intermittent, variable energy. Demand response counteracts this variability by managing use of energy based on available supply thus enabling a more sustainable, resilient, and reliable electricity grid. Since building energy use constitutes 20% of global delivered energy consumption and buildings use 75% of U.S. electricity [2], energy-efficiency and DR control of buildings can support the transition to clean energy and reductions in greenhouse gas emissions.

Advanced heating, ventilation, and air-conditioning (HVAC) systems, connected lighting, dynamic windows, occupancy sensing, distributed generation, and electrical and thermal energy storage are among many of the available building technologies that can be integrated and controlled to provide DR flexibility [3]. HVAC and lighting energy uses constitute 38% of total commercial building electricity use and 43% of the use occurs during weekday peak periods from 14:00 to 20:00 [4]. Since these end uses represent such a large percentage of the peak period load, strategies involving direct management (e.g., changing setpoints, switching off equipment) and indirect management (e.g., reducing cooling or heating loads, use of daylight) of these end uses are of high relevance. Impact estimates provided by the U.S. Department of Energy [5] indicate that a controls measure that enables a 20% shed of peak period HVAC, lighting and plug loads would avoid 196 TWh of annual electricity use, reduce average peak summer demand by 46 GW and save $10 billion in total U.S. building energy costs.

Dynamic windows modulate incoming solar radiation via chromogenic or mechanical means and can provide substantial demand side management services if integrated with related building systems. Dynamic windows include switchable, electrochromic (EC) glass coatings that can be actively modulated from a clear to tinted state with a small

* Corresponding author.
E-mail address: cgehbauer@lbl.gov (C. Gehbauer).

https://doi.org/10.1016/j.enbuild.2023.113481
Received 28 April 2023; Received in revised form 4 August 2023; Accepted 21 August 2023
Available online 8 September 2023

applied electric potential. When combined in an insulating glass unit with a low-emittance (low-e) coating, the resultant EC window can modulate both solar and visible transmission over a broad range. Hence, EC windows can be controlled to affect both cooling and heating loads and daylight admission in buildings while preserving a transparent view to the outdoors. There are numerous sputter deposition metal oxide EC windows available on the market, with alternate sol-gel room temperature solution-processed devices under development that promise to be of lower cost to manufacture [6] and [7]. Exterior motorized shading (or shading within closed cavity facades or ventilated double facades) provide a similar broad modulation of window heat gains and daylight, but without maintaining outdoor views. Controllable, thermally anisotropic materials are under development for the opaque envelope [8], and there are anisotropic solar control materials for windows that could be engineered to provide dynamic control as well [9].

Dynamic windows and shading, collectively referred to as dynamic facades, enable two types of load flexibility: 1) reduction of lighting energy use through daylighting, and 2) shift of HVAC loads to less critical periods of the day through appropriately timed admission or rejection of solar heat gains in support of HVAC thermal energy or electrochemical storage strategies. In prior studies evaluating the effectiveness of HVAC pre-cooling strategies of the building's thermal mass, proper control of window loads was assumed to occur through the use of exterior shading or other equivalent technologies [10], [11], and [12]. Pre-cooling strategies achieve demand savings through trade-offs between utility cost savings and occupant comfort, i.e., indoor temperature setpoints are often exceeded [13] and [14]. To minimize discomfort, prior studies reduced peak loads in perimeter zones with idealized automated shading without due consideration of visual comfort and daylighting requirements. In [15], a comprehensive evaluation of the demand side potential of thermostat, shading, and lighting demand-limiting controls in small commercial buildings was performed to identify promising applications by building types, climates, and utility rate incentives. The thermostat setpoint upper limit was increased to 24.4 °C during occupied periods, lighting was reduced by 20% during demand limiting periods, and estimated solar heat gains were reduced by 50%. The lighting and solar gain limitations were implemented on the ten highest air-conditioning demand days of the year. Total demand savings for a small office building were approximately 5 to 15 W/m^2 with time-of-use tariffs, where up to 2.2 W/m^2 were attributed to lighting demand-limiting controls. Demand savings and improvements to thermal comfort due to shading however were not disaggregated for the parametric dataset.

All of these prior studies demonstrated implicitly the importance of active control of facade loads in achieving load flexibility. Further work has been conducted to quantify the added value of dynamic facades, where control of the facade is explicitly modeled and practical considerations of comfort and indoor environmental quality related to the facade are included. Initial studies however were limited due to computational challenges. In [16], model predictive control (MPC) of an indoor or outdoor venetian blind and a thermally massive chilled radiant slab was simulated using offline optimization with reduced order models and a linear 24 h predictive programming solution. In [17], dynamic windows were evaluated for a south-facing perimeter office under sunny summer and winter conditions in two temperate climates. Model predictive control was implemented using non-linear programming (NLP), which is designed to find local solutions for constrained non-linear problems. The scope of both studies was constrained significantly by computational limits of the optimization solver and complexity of implementation. Modeling one week of control for a single zone (5 min time step, 24 h prediction horizon) for the latter study, for example, took over a day to compute on a high-performance cluster computer when the NLP solver was used.

Given related work on building-to-grid controls integration, the accuracy and ease of numerical simulations were increased through redesign of our modeling workflow [18]. Hence in this study, control was implemented with mixed-integer linear programming (MILP) which poses a significant advantage over the previously used NLP implementation, as it guarantees mathematical convergence to a global optimum, i.e., best control for the multiple objectives, and accommodates both discrete and continuous variables. Window solar-optical states were modeled as discrete with the exact numeric value rather than approximated with a nonlinear function (with the NLP approach), enabling more realistic estimations of DR potential. The MILP solving times were significantly reduced from about 90 s in the NLP implementation to a median of about 2 s with MILP. This rapid convergence not only benefits the simulation evaluation, but also enables future real-time control of dynamic facades and HVAC systems by quickly adapting to changing environmental conditions; e.g., by preventing immediate glare during dynamic sky conditions or dampening future window actuation based on forecast knowledge. Annual evaluations of DR control were also made feasible within practical time limits, enabling exploration of technical potential across a wide range of conditions. Computation times per MPC case were reduced from about 40 days for a single simulated year to about one day by utilizing the parallel architecture of Lawrence Berkeley National Laboratory's Lawrencium High Performance Computing Cluster and speedups in underlying algorithms.

Table 1
Overview of control strategies.

Case	Facade type	Facade control	Thermostat
Reference	Shade	Static	Schedule
Heuristic-EC	Electrochromic	Heuristic	Schedule
MPC-EC	Electrochromic	MPC	Schedule
MPC-EC&HVAC	Electrochromic	MPC	MPC

The objective of this study is to estimate the magnitude of impact that integrated dynamic facades can have as an efficiency and load flexibility measure at a national scale and convey how such impacts vary with regional and temporal variability in grid conditions. Such technical-economic studies across a range of climates and tariffs are used to inform policy, stakeholder investments, and regional market analysis in support of climate change decarbonization goals. With the computational advancements described above, numerical annual simulations of a prototypical medium office building were performed at an unprecedented level of resolution (i.e., 5 min time step and 24 h prediction horizon). Dynamic facades with and without integration with the HVAC system were modeled to minimize energy cost and address critical market acceptance issues (thermal comfort, glare, daylight, and view related to indoor environmental quality, health, and wellness). DR potential and price sensitivity were assessed through conventional flat and time-variable tariff schedules across all 16 U.S. climate zones. No prior study encompasses the depth and breadth of this analysis. Unique aspects of this study include use of advanced ray-tracing models for window heat gain, daylight, and comfort performance within the MPC controller and building emulator and an advanced optimization workflow that identifies global optimum control states. Potential co-benefits and technical limitations are discussed.

2. Methodology

In this study DR controls were used to minimize energy cost while meeting visual and thermal comfort requirements. This was accomplished using dynamic windows, dimmable lighting, and a controllable thermostat. Existing flat and time-of-use utility rate schedules were applied to instigate DR control under emerging grid conditions. Performance was assessed using simulations of a prototypical medium office building across all 16 U.S. climate zones [19] and five tariffs. One reference and three control cases were evaluated, see Table 1. The Supplemental Materials include details of the simulation model, control cases, climate zones, and tariffs.

For two cases, the dynamic windows were controlled with heuristic or MPC algorithms independent of the thermostat. The heuristic control

Table 2
Inputs and outputs of MPC controller.

Variable	Description	Unit	Source
dt(t)	Date and time of year	–	Forecast
DNI(t)	Direct normal irradiance	W/m^2	Forecast
DHI(t)	Diffuse horizontal irradiance	W/m^2	Forecast
T_{out}(t)	Outdoor dry-bulb temperature	°C	Forecast
P_{equip}(t)	Equipment power use	W	Prediction
Q_{occ}(t)	Sensible occupant load	W	Prediction
T_{in}	Room air temperature	°C	Measurement
T_{slab}	Slab temperature (optional)	°C	Measurement
DGP_{limit}(t)	Daylight glare probability limit	1	Setting
I_{set}(t)	Workplane illuminance setpoint	lx	Setting
R_{energy}(t)	Rate for energy	$/kWh	Setting
R_{demand}(t)	Rate for demand	$/kW	Setting
$T_{set\text{-}heat}$(t)	Thermostat heating setpoint	°C	Setting
$T_{set\text{-}cool}$(t)	Thermostat cooling setpoint	°C	Setting
$\nu_{lighting}$	Lighting power efficiency	W/lx	Setting
μ	HVAC heating efficiency	1	Setting
cop	HVAC cooling coefficient of performance	1	Setting
$Q_{HVAC\text{-}limit}$	HVAC power limit	W	Setting
u(n)	Dynamic window tint state per zone *n*	1	Output
$T_{set\text{-}heat/cool}$	Thermostat heating/cooling setpoint override	°C	Output

refers to state-of-the-art commercial control systems which are typically based on control logic (if/then rules) in response to sensor inputs. More detail on the control cases is given in S.3 Control Cases. For the third case, MPC HVAC thermostat control was coupled with dynamic window control. Performance was compared to a conventional reference case with a dual-pane, spectrally-selective, low-e window with an indoor roller shade. In all control cases, the electric lighting was dimmed or shut off in response to available daylight or occupancy. More detail on the simulation method is given in S.1 Simulation Method for Evaluation.

The general aim of DR control is to extract the maximum demand reduction from the system for the lowest capital investment. With dynamic windows, however, the technology provides other energy and non-energy co-benefits, so DR control was constrained by occupant requirements: no increase in deadband temperature range, reduction in lighting setpoint, or violation of visual comfort. Also, only the associated incremental cost of implementing DR was used in the assessment.

2.1. MPC control

The MPC controller was defined within the Distributed Optimal and Predictive Energy Resources (DOPER) controller environment, which is an open-source package for optimal control in the context of smart inverter, battery storage, and distribution grids [18]. DOPER was extended with detailed thermal zone, dynamic facade, and occupant comfort models. The dynamic facade controller was first introduced in [17] and adapted to the DOPER framework using a mixed-integer linear implementation. The full MPC implementation used in this study is publicly available through the Advanced Fenestration Control[1] package.

With MPC, a model of system operation, along with forecasts of weather and disturbances, is used to predict future performance and optimize setpoint schedules and/or control setpoints over a specified time horizon. The solution of the first control step is applied to the system and the optimization is solved again with updated information of system state and forecasts for the next control step. The MPC algorithm for this study minimizes the perimeter zone energy cost per 5 minute control step over a forecast horizon of 24 hours, within visual and thermal comfort constraints. The inputs to the MPC controller for each timestep, t, are weather and other forecasted quantities, sensor data, and configuration parameters. A detailed description for each input and output is given in Table 2 and a controller block diagram is given in Fig. 1.

[1] Advanced Fenestration Control (AFC): https://github.com/LBNL-ETA/AFC.

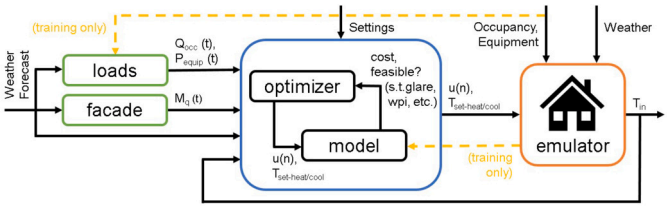

Fig. 1. Controller block diagram with 24 hour weather forecast data feeding the prediction of internal loads (equipment and occupancy) and facade model, shown in green outline, feeding the model predictive controller, blue outline, with its interaction between the optimization model and numeric optimizer, and further feeding the control outputs of tint state per zone, u(n), and (optionally) thermostat heating and cooling setpoint override, $T_{set\text{-}heat/cool}$, to the emulator, orange outline. Additional inputs include settings for the controller, and data for current occupancy, equipment load, and weather for the emulator. During training/development of the controller, data from the emulator is passed to the load prediction and optimization models, illustrated by yellow arrows.

The discrete tint states of the electrochromic windows are implemented as a table with binary lookup variables, shown in Equations (1) and (2).

$$z_q(t) = \sum_{n=1}^{f} \sum_{s=1}^{a} M_q(n, s, t, dt(t), DNI(t), DHI(t)) * b_{state}(n, s, t) \quad (1)$$

subject to

$$\sum_{s=1}^{a} b_{state}(n, s, t) == 1 \quad (2)$$

Each quantity supplied by the dynamic facade, z_q, is derived from the corresponding Radiance model, M_q, through a binary lookup variable, b_{state}. The Radiance model is introduced in Section 2.2. The lookup is performed by summing quantities for all tint states, s, and all window zones, n, subject to the binary lookup variable. In order to allow only a single tint state per zone, Equation (2) limits b_{state} to a sum of 1 across the possible tint states. For this study the number of discrete tint states, a, was four and the number of window zones, f, was three. The quantities, q, are vectors of the following:

- daylight: three-phase method for daylight illuminance for a grid (1×1 ft in this study) of workplane points [20]
- vil: three-phase method for vertical illuminance at the occupant eye level (1.5 m centered, parallel to the window in this study) as input to DGPs [20], [21]

- abs: a three-phase method for incident irradiance on each of the window glass layers [16] [22]
- tra: a three-phase method for incident irradiance on each of the room surfaces [16] [22]

The objective for MPC control is defined in Equations (3) to (7).

$$\min \sum_{t=1}^{h} c_{energy}(t) + c_{demand}(t) + \rho_{view}(t) + \rho_{actuation}(t) \tag{3}$$

subject to

$$DGPs(z_{vil}(t)) \leq DGP_{limit}(t) \tag{4}$$

$$z_{daylight}(t) + I_{lighting}(t) \geq I_{set}(t) \tag{5}$$

$$T_{set-heat}(t) \leq T_{in}(t) \leq T_{set-cool}(t) \tag{6}$$

$$Q_{HVAC}(t) \leq Q_{HVAC-limit} \tag{7}$$

The cost for energy, c_{energy}, cost for demand, c_{demand}, and penalties for outdoor views, ρ_{view}, and facade actuation, $\rho_{actuation}$, for each timestep, t, over the optimization horizon, h, is minimized. The glare level is determined by the vertical illuminance, z_{vil}, and converted to DGPs and constrained to the DGP limit. The desired workplane illuminance level is defined by I_{set} and provided by the available daylight, $z_{daylight}$, and artificial lighting, $I_{lighting}$. The ambient air temperature, T_{in}, is constrained to reside within the heating, $T_{set\text{-}heat}$, and cooling, $T_{set\text{-}cool}$, thermostat setpoints. The HVAC system is constrained by a maximal capacity, $Q_{HVAC\text{-}limit}$. For the cases with HVAC control, the MPC controller can narrow the thermostat setpoints, if desired, but it cannot exceed them.

The energy cost functions are defined in Equations (8) to (13).

$$c_{energy}(t) = P_{total}(t) * R_{energy}(t) \tag{8}$$

$$c_{demand}(t) = \Delta \sum_{j=1}^{m} max(P_{total}(t) \forall t \in p(j)) * R_{demand}(j) * w_{demand} \tag{9}$$

where

$$P_{total}(t) = P_{lighting}(t) + P_{HVAC}(t) + P_{equip}(t) \tag{10}$$

$$P_{lighting}(t) = I_{lighting}(t) * \nu_{lighting} \tag{11}$$

$$P_{HVAC}(t) = \begin{cases} Q_{HVAC}(t) * cop & \text{if } Q_{HVAC}(t) \leq 0 \\ Q_{HVAC}(t) * \mu & \text{else} \end{cases} \tag{12}$$

$$T_{in}(t), T_{slab}(t) = M_{RC}(T_{in}(t-1), T_{slab}(t-1), T_{out}(t-1), P_{equip}(t-1), Q_{occ}(t-1), Q_{HVAC}(t-1), P_{lighting}(t-1), z_{abs}(t-1), z_{tra}(t-1)) \tag{13}$$

The cost for energy, c_{energy}, is defined by the temporal total electricity demand, P_{total}, and the applicable utility rate for energy consumption, R_{energy}. The cost for peak demand, c_{demand}, is computed by the maximal total electricity demand for each of the demand periods, p, the applicable utility rate, R_{demand}, and a weighting factor, w_{demand}, to scale monthly demand cost to daily energy cost, e.g., divide demand cost by 22 days. The total electricity demand is the sum of lighting power, $P_{lighting}$, HVAC power, P_{HVAC}, and internal equipment power, P_{equip}. The electric lighting power is defined by the demand for artificial lighting, as determined by Equation (5), subject to the lighting power efficiency, $\nu_{lighting}$, which defines a linear relationship of electric power versus light output, see Table 3. The electric HVAC power is computed from the sensible HVAC power, Q_{HVAC}, with a fixed efficiency for cooling and heating. The ambient and slab temperatures are derived from a grey box resistance-capacitance thermal model, M_{RC}. The inputs to the RC model are ambient and slab temperatures of the previous timestep, outdoor dry-bulb temperature, internal equipment power use, sensible occupant load, sensible HVAC power, lighting power, and vectors of absorbed and transmitted solar irradiation, z_{abs} and z_{tra}, for the respective window layers and room surfaces. The parameters for resistors and capacitors of the M_{RC} model were dynamically tuned at runtime, i.e., every two days in this study, with respective observations from the emulator. See [17] for method of calculation. The predicted room air temperature from the MPC controller is converted to thermostat cooling and heating setpoints using a pre-defined deadband of 0 and 0.2 K respectively when pre-cooling and 0.2 and 0 K respectively when pre-heating. Otherwise, the setpoints passed to the building are not changed, i.e., follow the time of day setpoint schedule.

Table 3
Medium office prototype characteristics.

Prototype	Medium office building; new construction; 4,982 m^2 floor area
Perimeter zone	3.1 m (10 ft) wide; 4.6 m (15 ft) deep; 2.7 m high (9 ft) 28.3 offices each in east and west perimeter 44.6 offices each in north and south perimeter
Core zone	same dimensions as perimeter; 211.7 offices total
Occupant load	18.6 m^2/person seated person: 73.3 W (sensible) based on DOE reference schedules
Equipment load	10.8 W/m^2 based on DOE reference schedules
Lighting load	10.8 W/m^2; 0.017 W/m^2lx
Window-to-wall ratio	40%
Reference window	SHGC = 0.40; Tvis = 0.62; U-value = 1.6 W/m^2K interior shade; black fabric; 2% openness factor 80% lowered all year
Electrochromic window	3 equally sized horizontal zones; 4 control states SHGC (clear to dark): [0.42, 0.16, 0.12, 0.10] Tvis (clear to dark): [0.60, 0.18, 0.06, 0.01] U-value = 1.6 W/m^2K
Thermal mass	10.1 cm (4 in) thick concrete slab
Lighting controls	300 lx with daylight dimming (0–100%) vacancy control based on DOE reference schedules
HVAC system	cooling: 24.0–26.5 °C; heating: 15.5–21.0 °C setpoints based on DOE reference schedules COP = 3.23; heating efficiency = 0.8
Occupant viewpoint	parallel to window due right; room centered 1.5 m from window; 1.2 m height

The penalty functions are defined in Equations (14) to (16).

$$\rho_{view}(t) \geq \sum_{n=1}^{f} [max(A_{state}(s) \forall s \in \{1, \ldots, a\}) - u(n,t)] * w_{view} \tag{14}$$

$$\rho_{actuation}(t) = \sum_{n=1}^{f} \| \Delta u(n,t) \| * w_{actuation} \tag{15}$$

where

$$u(n,t) = \sum_{s=1}^{a} A_{state}(s) * b_{f\,state}(n,s,t) \tag{16}$$

Penalties are mathematical formulations to enforce desired behavior of the MPC control. The desire to keep an unobstructed view towards the outdoors is implemented with a view penalty for the difference between the most clear tint state, defined by the maximum of all tint states A_{state} for all states, a, and the current tint state, u. The weighting factor w_{view} is added to trade-off view versus energy and demand cost. Another penalty is implemented to reduce the actuation of the dynamic facade to limit occupant disturbance. The absolute of the derivative of the tint state is penalized with a weighting factor, $w_{actuation}$. The current tint state is determined with the lookup table, A_{state}, and the binary lookup variable. Note that in order to evaluate the technical potential, only the actuation penalty was used in this study.

Table 4
Overview of tariffs for summer season.

	Weekday peak price [$/kW]				Weekday period		
Name	All time	off-peak	on-peak	on/off ratio	Months	off-peak	on-peak
TOU-high	21.1	0.0	21.9	2.0	May-Nov	22-8 h	12–18 h
TOU-low	0.0	2.4	14.8	6.2	Jun-Oct	21-9 h	9–21 h
TOU-late	12.4	0.0	32.1	3.6	May-Oct	21-16 h	16–21 h
Flat-high	3.8	0.0	0.0	1.0	all year	all day	–
Flat-low	14.8	0.0	0.0	1.0	Jun-Oct	all day	–

2.2. Performance evaluation

Building energy use was emulated using a Modelica[2] building physics model to determine the window and room heat balance, Radiance[3] three-phase method for solar radiation and daylight illuminance levels, Radiance five-phase method [23] for glare analysis (enhanced simplified daylight glare probability, eDGPs [21]), and Python-based tools to manage input data, such as weather data and occupancy schedules. Control setpoints were determined interactively with the emulator through a timestep-to-timestep interactive co-simulation at each five minute timestep. Forecast data were generated directly from simulated weather data without forecast uncertainty. A detailed description of the simulation model is given in S.2 Description of Building Prototype.

The U.S. Department of Energy (DOE) prototypical medium office building [24] was modeled using four perimeter cellular offices and one core zone. The prototype was modified to include dual-pane windows and daylight dimming controls. Scheduled equipment and occupant loads were the same for all modeled cases. Salient building characteristics are summarized in Table 3. Results were scaled to a whole building assuming adiabatic conditions between zones. Parametric simulations were performed to evaluate DR performance, totaling 1,280 conditions. The conditions include all 16 U.S. climate zones, five tariffs introduced in Table 4, one reference, and three test cases introduced in Table 1. Detailed descriptions are given in the Supplementary Materials.

At the perimeter zone level, annual critical peak electricity demand savings were computed based on the maximum non-coincident 15-min peak load that occurred during the critical on-peak demand period defined by the TOU-high tariff, i.e., the on-peak period on weekdays from 12:00 to 18:00 for the summer period (May through October). The TOU-high tariff is indicative of when DR reductions across the grid are most needed, as represented by the stringent price difference between off- and on-peak periods. The TOU tariffs specify stacked prices for the peak demand, which consist of the all-time monthly peak and the peak during the on- or off-peak periods. For example the total cost for TOU-high with a peak during the off-peak period would be 21.1 $/kW plus 0.0 $/kW which equals 21.1 $/kW, and during the on-peak period it would be 21.1 $/kW plus 21.9 $/kW which equals 43.0 $/kW, and results in a cost ratio between on- and off-peak of 2.0.

All cases were evaluated based on the maximal peak demand during this critical on-peak period. This evaluation method enabled equitable comparisons between load shapes resulting from the three control strategies. Non-coincident demand savings were determined by the whole summer period in which the reference or test case peak load occurred (e.g., reference: July 7 at 16:45; test case: August 21 at 16:00). Note, to compute the peak, all load profiles were resampled to a typical utility accounting period of 15 minutes. The simulation timestep was 5 minutes, hence the hourly load schedules and hourly weather data were linearly interpolated. For whole building demand savings, load profiles for the perimeter zones and core zone were scaled and summed on a temporal basis, resulting in a whole building load profile for each 15 min time step of the critical period. Critical peak demand savings were computed using the same methods used at the perimeter zone level. Coordinated control between perimeter zones or the central plant was not implemented in this study, so whole building demand reductions represent a conservative estimate.

The HVAC thermostat schedule was not ramped, i.e., the whole building was set to occupied when DOE prototype occupancy factors were greater than 10%. Equipment and occupant load schedules were ramped based on the DOE prototype schedules. Numerical implementation of the algorithms is described in detail in [17]. Physical implementation and testing of earlier MPC prototypes is described in [25].

3. Results

The data was analyzed for individual perimeter orientations and at the whole building level, where perimeter and core loads were aggregated to a whole building equivalent to the DOE medium office prototype. See Section 2.2, Table 3, and the Supplementary Materials for more details. All data is reported as site energy. The results section is structured based on the four core metrics:

- Peak Demand Savings: The annual non-coincident peak demand is defined as the highest 15-min average electricity demand for the most critical period. The most critical period is defined as the TOU-high tariff's most expensive on-peak period on weekdays from 12:00 to 18:00, May through October.
- Energy Cost Savings: The annual energy cost is the resulting electricity cost for each of the tariffs shown in Table 4 and cost for natural gas from heating demand. The electricity cost includes the cost for energy and peak demand, where applicable. The cost for natural gas was taken from the individual DOE medium office prototype buildings for each of the 16 climates.
- Electricity Savings: The annual electricity consumption is the sum of all electricity demand throughout the year.
- Emission Savings: The annual greenhouse gas (GHG) emissions are defined by the combined carbon dioxide (CO_2) equivalent emissions. Electricity emission factors include combustion and precombustion for the 2030 mid-case scenario with 95% decarbonization by 2050 as provided by the Cambium tool [26]. Emissions from natural gas are computed with a 14.4 kg CO_2-equivalent per MMBtu, per U.S. Environmental Protection Agency report [27]. See the Supplemental Materials for more information.

The results section first provides an overview of the benefits at the building level, Fig. 2 and individual perimeter level, Fig. 3, followed by subsections for each of the core metrics. The Appendix provides a full overview of the building-level savings. Individual perimeter results are provided on request.

3.1. Critical peak demand savings

At the whole building level the annual peak demand savings for the TOU-high tariff are evenly distributed across the 16 climate zones, see Fig. 2 and Table 5. Reductions from the three control scenarios across all climates complement each other, with median savings of 6.6% for Heuristic-EC, MPC-EC more than doubling the savings to 14.0%, and

[2] https://modelica.org/.
[3] https://www.radiance-online.org/.

Table 5
Critical peak demand savings across five tariffs and sixteen climates.

Orientation	Unit	Heuristic EC			MPC EC			MPC EC & HVAC		
		min	med.	max	min	med.	max	min	med.	max
South	%	14.3	20.2	27.0	29.2	36.4	44.2	29.4	40.7	49.7
	W/m^2	5.0	7.8	10.8	10.3	13.9	17.6	10.5	15.9	19.8
West	%	23.2	31.1	34.6	33.2	44.6	51.3	33.3	46.8	55.4
	W/m^2	7.6	12.3	13.7	13.2	17.4	19.9	13.3	17.9	21.9
East	%	4.1	8.8	14.5	0.7	29.6	37.4	12.5	32.4	41.6
	W/m^2	1.1	2.4	4.5	0.2	8.5	11.6	3.5	9.3	12.2
North	%	10.0	17.1	20.5	10.5	25.0	32.7	10.8	27.6	39.7
	W/m^2	2.7	4.3	5.4	2.8	6.8	8.8	2.9	7.3	10.8
Building	%	3.4	6.6	8.5	8.0	14.0	15.8	8.2	15.7	19.8
	W/m^2	0.9	1.9	2.4	2.3	3.9	4.4	2.4	4.4	5.6

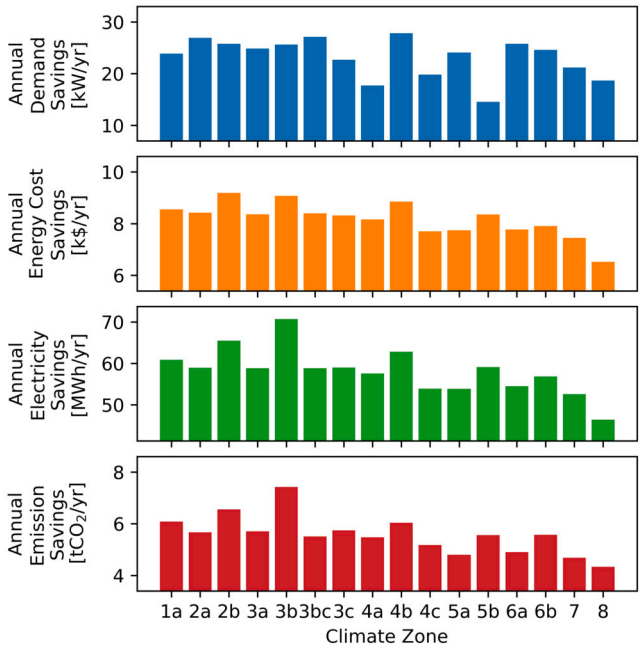

Fig. 2. Savings at the medium office building level for the TOU-high tariff across the 16 climate zones with integrated MPC-EC&HVAC control strategy. Annual non-coincident demand savings in kW (blue), energy cost savings in k$ (orange), electricity savings in MWh (green), and emission savings in tCO_2 (red).

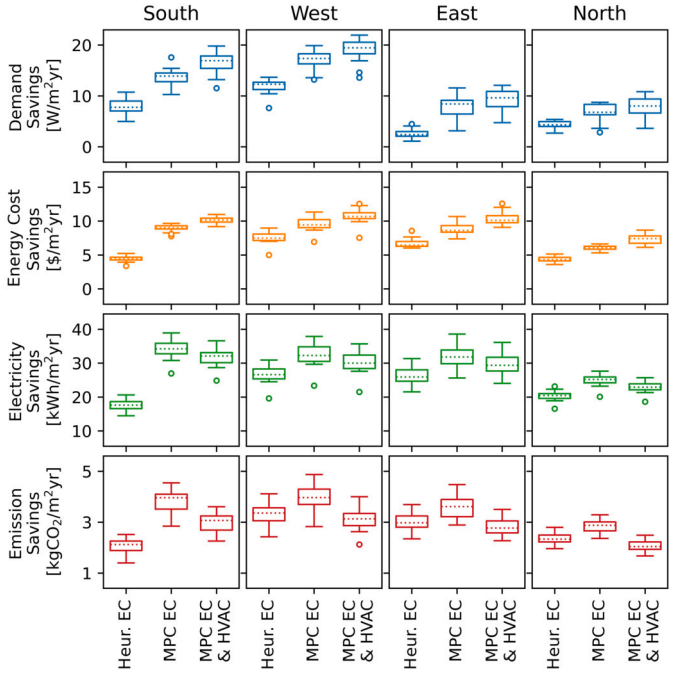

Fig. 3. Savings at the perimeter level across the 16 climate zones and five tariffs. The three control strategies Heuristic-EC, MPC-EC, and MPC-EC&HVAC are shown on the x-axis. The columns of subplots correspond to the cardinal perimeter orientations and the rows of subplots correspond to the four core metrics.

marginal improvement to 15.7% for integrated MPC-EC&HVAC control. Further analyzing the per-climate savings for the TOU-high tariff and integrated MPC-EC&HVAC scenario, Fig. 2, the savings range between 14.6 to 27.8 kW for the whole medium office building, with climate zones 5b (Boulder, CO – cool and dry) and 4a (Baltimore, MD – mixed humid) at the bottom end and climate zones 4b (Albuquerque, NM – mixed dry) and 3bc (Los Angeles, CA – warm marine) at the top end.

At the perimeter level demand savings are more significant. The south and west facing perimeters showed the highest savings, with up to 45.8% and 52.0% peak demand savings, respectively, while the east and north perimeters showed savings up to 37.4% and 35.9%, respectively. Note that all normalized perimeter savings, i.e., peak demand reduction per square-meter floor space, were an order of magnitude higher than at the whole building level. For example, the maximal peak demand savings for a south-facing perimeter were 19.8 W/m^2 while at the building level the maximal demand reductions were only 5.6 W/m^2. This is due to the perimeter-to-core aspect ratio of the floor plate and facade orientations. The medium office building was modeled with a 1:1.5 perimeter-to-core aspect ratio, with the longer facades facing due north and south. The median whole building demand savings were about one quarter of those for individual perimeter zones, and maximal whole building savings were about three times lower than individual perimeter zone savings. These differences in magnitude of savings can be attributed to dilution of perimeter zone savings when aggregating the individual load profiles with the large core zone. Smaller, perimeter zone dominated buildings will have greater whole building demand savings.

It is important to understand how savings occur on a temporal basis. Fig. 4 illustrates the internal control mechanisms for a south-facing perimeter office on a sunny day in June. The first subplot shows the marginal difference in load demand, mainly in the early morning and late afternoon hours, between the shade reference case and the Heuristic-EC case. The peak demand during the peak period from 12:00 to 18:00 is equivalent. Adding smart controls through MPC-EC leverages the EC technology and drastically reduces both, the total energy and peak demand by about one third, illustrated as the shaded gray area. Integrating the MPC-EC&HVAC systems further reduces the daytime energy and peak demand by utilizing the pre-cooling strategy. Hereby

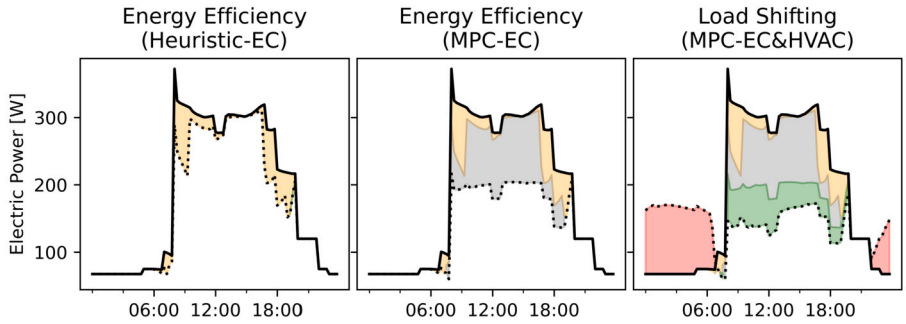

Fig. 4. 15 minute electric demand profiles, in W, on a clear sunny day in June, south-facing perimeter office, climate zone 3bc (Los Angeles, CA – warm marine), TOU-high. Left: shade Reference case, black solid line, and Heuristic-EC, dotted outline, with load reductions shaded in beige. Middle: MPC-EC control profile, dotted outline, with reductions due to MPC control of the EC window shaded in gray. Right: MPC-EC&HVAC control profile, dotted outline, with the load shift from the MPC-EC window and thermostat control for load reduction shaded in green and the load increase shaded in red.

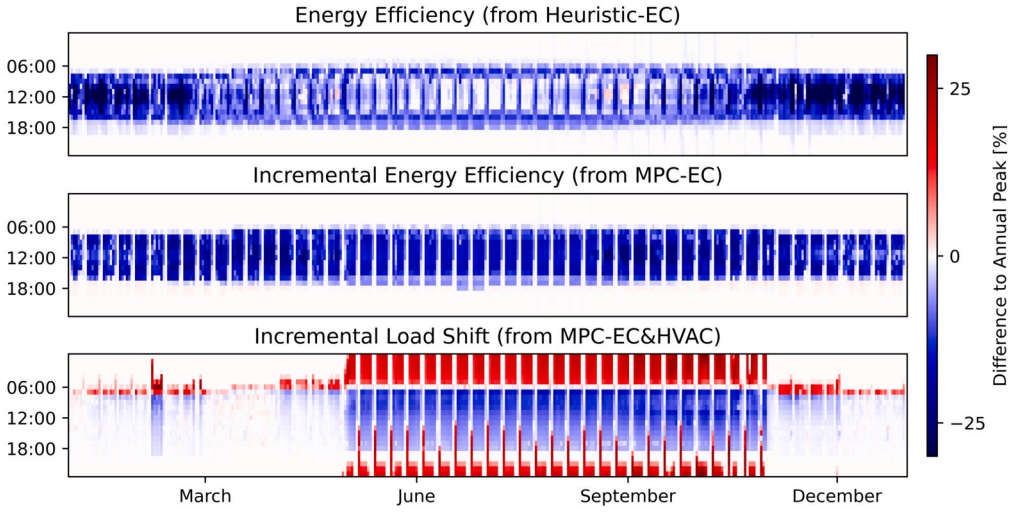

Fig. 5. Difference between hourly electric demand per time of day for the year, normalized by annual peak load (40.4 W/m^2 floor area) of the shade Reference case. South-facing perimeter office, climate zone 3bc (Los Angeles, CA – warm marine), TOU-high. Top: Normalized difference between the shade reference case and the Heuristic-EC control. Middle: Normalized difference between the Heuristic-EC control and the MPC-EC control. Bottom: Normalized difference between the MPC-EC control and the integrated MPC-EC&HVAC.

the HVAC system is controlled to reduce the temperature setpoint during the night to thermally charge the mass of the building, e.g., slab, furniture, walls, etc., shown as shaded red area, and then release the energy during the daytime to offset HVAC demand, shown as shaded green area. Given the reduced HVAC load, the EC windows can respond with brighter tint levels, permitting more daylight and offsetting electric lighting. Lighting and cooling loads are reduced to minimum levels, with the remaining load attributable to uncontrollable internal equipment.

Extrapolating this analysis for a full year, shown in Fig. 5, the transition from the shade reference case to the Heuristic-EC control yields diverse savings throughout the year. In winter this transition largely reduces consumption during the daytime, indicated as the dark blue area in the center line of the first subplot, and moderately reduces consumption in the morning and afternoon hours. Controversially, in summer the benefit of the Heuristic-EC case vanishes during the daytime, while moderate reductions during the morning and evening hours remain. This is consistent with Fig. 4 first subplot showing an example for a sunny day in June. On rare occasions during the transitional seasons the electricity demand is slightly increased, shown as lightly shaded red areas mainly around end of May and mid-August during the daytime. The transition to electrochromic windows does not alter the nighttime consumption, indicated by the white area, except for some rare occasions during the fall season where reduced daytime loads lead to less residual cooling demand in the evening hours. The incremental benefit of adding MPC-EC is shown in the second subplot. Savings are substantial and consistent throughout the year, indicated by the consistent dark blue area, which is again consistent with the second subplot in Fig. 4. The highest savings occur during the transitional seasons at mid-day. The last subplot shows the incremental benefit of integrating MPC-EC&HVAC. It can be seen that for the summer period the controller utilizes the pre-cooling strategy illustrated in the last subplot in Fig. 4, where thermal mass is charged at night, indicated by greater electricity demand in the late night and early morning hours shown in red, and released during the daytime, indicated by the reduced demand in blue. The vertical white gaps without load alternation indicate weekends where the controller does not request pre-cooling. However, on Sunday afternoons the controller typically starts to pre-cool and prepare for the upcoming occupancy and solar gains on Monday. On the other hand in the winter season pre-cooling is utilized to a much lesser degree, with a load increase lasting only for a few hours instead of all night, as it is in the summer. An example of the thermostat and tint patterns for the three electrochromic control cases is given in the Appendix with Figs. A-1 and A-2.

To illustrate the stable control that MPC can provide across a range of weather conditions, load conditions, and climates, Fig. 6 illustrates the daily peak demand for each day of the critical period, i.e., May through October for both the TOU-high tariff with peak period from 12:00 to 18:00, left column of plots, and the TOU-late tariff, with a peak period from 16:00 to 21:00, right column of plots. The daily peak

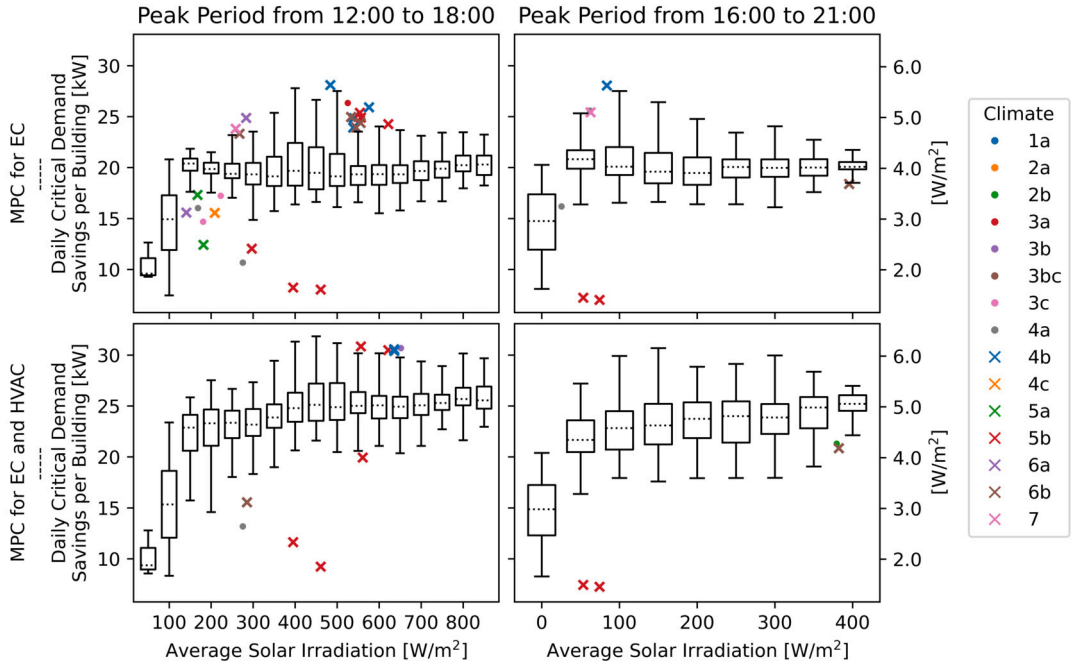

Fig. 6. Daily whole building peak demand savings, defined by the TOU-high tariff (May through October) from 12:00 to 18:00 (left plots) and for the TOU-late tariff from 16:00 to 21:00 (right plots) between the shade Reference case versus MPC-EC (upper plots) and MPC-EC&HVAC (lower plots). The primary y-axis shows absolute savings, the secondary y-axis shows a second scale with savings normalized by the building floor area. Average daily global horizontal solar irradiation (W/m^2) over the peak period is binned in 50 W/m^2 increments and shown on the x-axis. Outliers are colored by climate zone.

is plotted versus the average global horizontal solar irradiation (GHI) during the peak period. It can be seen that the daily critical load reductions were fairly insensitive to varying weather conditions and the two critical peak periods. Significant critical peak demand reductions occurred on both cloudy days, when solar GHI was low and the expected renewable energy output was reduced and there was a higher dependency on electrical energy storage, and on sunny days, when the GHI was high. Outlier data with reduced savings is colored based on the climate zone. Note that an intermittent reduction in peak demand savings can be caused by weather conditions or poor control decisions of the MPC, but it does not necessarily propagate to annual demand savings. For example, the climate zone 5b (Bolder, CO – cool dry) had two outliers between the 400 and 500 W/m^2 average GHI, each marked as a red x, for both the MPC-EC and MPC-EC&HVAC cases. These outliers momentarily decreased the daily demand savings from about 25 kW to 10 kW. However, the total building demand of 118.9 kW for this day remained significantly lower than highest annual critical peak of 129.1 kW for the MPC-EC&HVAC case, and therefore the impact of such outliers were negligible. When solar GHI levels were very low, demand savings decreased. However, most climates in the U.S. represent a cooling-driven peak for the DOE medium office building typically and are driven by days with high solar GHI and temperatures. The reduced peak demand savings during low solar GHI days are of less relevance in support of the electric power grid. Savings of the dynamic facade system remained apparent even after sunset, i.e., when average GHI was near zero, due to dynamic solar control to decrease residual HVAC load and manage daylight to offset electric lighting.

The five different tariff schedules applied in this study represent different structures, with and without time-varying rates, and with and without critical peak demand charges. Fig. 7 illustrates the price-responsiveness as a result of these structural and magnitudinal differences as incremental energy and demand savings across the three control cases. For energy savings, in the upper row of plots, the load shift strategy through pre-cooling is apparent for most of the MPC-EC&HVAC tariffs, except the Flat-high tariff. During the off-peak time, first subplot, energy savings are negative, i.e., pre-cooling leads to increased demand in comparison to the MPC-EC case. This allows for decreased energy demand during the mid-peak and on-peak periods, see middle and right subplots. The magnitude of energy increase during the off-peak time determines the energy shifted, and therefore the

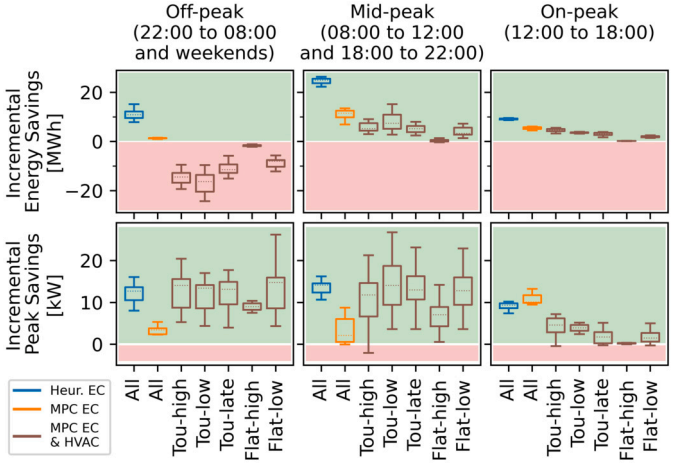

Fig. 7. Price responsiveness with different tariff schedules on building level energy demand, in MWh, (upper plots) and non-coincident peak demand, in kW, (lower plots) savings for three control cases across the 16 U.S. climate zones. Box-plots are shown as an incremental benefit between the shade reference, Heuristic-EC (blue), MPC-EC (orange), and MPC-EC&HVAC (brown) cases. The savings are shown for the summer season defined by the TOU-high tariff (May through October) and for three periods of off-peak from 22:00 to 08:00 weekdays and all day weekends (left column), mid-peak from 08:00 to 12:00 and 18:00 to 22:00 (middle column), and on-peak from 12:00 to 18:00 (right column). Load or energy use reductions, where savings are positive, are indicated by the shaded green area and increases, where savings are negative, are indicated by the shaded red area. The x-axis shows the results for the specific tariff. Note that load profiles that originated from the five different tariff schedules were re-evaluated based on the TOU-high periods. Results for the Heuristic-EC and MPC-EC cases did not vary with tariff and are marked with "All".

Table 6
Energy cost savings across five tariffs and sixteen climates.

Orientation	Unit	Heuristic EC			MPC EC			MPC EC & HVAC		
		min	med.	max	min	med.	max	min	med.	max
South	%	11.6	16.8	20.6	25.4	32.0	35.6	27.2	33.8	38.5
	$/m^2	1.2	1.8	5.2	2.3	3.4	9.7	2.5	3.6	11.0
West	%	18.6	26.3	31.6	24.4	34.0	38.5	23.9	36.5	41.6
	$/m^2	1.4	2.7	9.0	1.9	3.4	11.3	2.0	3.8	12.5
East	%	22.0	24.8	30.2	23.4	31.9	38.7	26.6	36.2	44.4
	$/m^2	2.0	2.7	8.6	2.3	3.6	10.7	2.7	4.1	12.6
North	%	13.6	18.2	21.3	20.9	24.7	27.6	20.4	26.7	33.6
	$/m^2	0.9	1.9	5.2	1.5	2.4	6.6	1.5	2.4	8.7
Building	%	6.7	8.1	8.7	9.2	11.4	12.9	8.6	11.2	13.5
	$/m^2	0.2	0.7	1.2	0.3	0.9	1.8	0.3	0.9	1.8

achieved energy reduction in the subsequent periods. This is a complex relationship between the underlying building plug load and HVAC demand, occupancy, weather conditions, as well as the tariff structure and cost magnitudes. For example, the TOU-low tariff leads to the highest increase during off-peak and the highest decrease during mid-peak. However, the energy savings during the most expensive on-peak period are lower than these for the TOU-high tariff. This is due to the control decision when and how long to pre-cool and how to release the thermal mass, see also Fig. 5. Even though energy demand is increased, the MPC controller is able to manage and optimize the demand to avoid increasing the monthly and annual peak demands. For all cases the MPC controller is able to decrease the peak demand while increasing the energy consumption for pre-cooling during the off-peak period. Based on the amount of pre-cooling provided, the critical peak demand during the on-peak period, last subplot in the lower row of plots, is reduced accordingly. It can be seen that the TOU-high tariff leads to highest incremental critical peak demand savings for the MPC-EC&HVAC case over the MPC-EC case with reductions up to 7.5 kW (Los Angeles, CA – warm marine) followed by TOU-late with up to 6.9 kW (Duluth, MN – very cold). The TOU-low and Flat-low tariffs lead to equivalent savings of up to 5.2 kW, and Flat-high tariff leads to savings of up to 2.2 kW.

3.2. Annual energy cost savings

At the whole building level the annual energy cost savings for the TOU-high tariff are equivalent for most of the 16 climate zones but they tend to decrease in colder climates such as climate zones 7 (Duluth, MN – very cold) and 8 (Fairbanks, AK – subarctic), see Fig. 2 and Table 6. The median energy cost savings for replacing the shade reference case with the heuristically controlled ECs are 8.1% or 0.7 $/m^2. While median savings for the MPC-EC case significantly increase to 11.4%, the MPC-EC&HVAC case shows similar median savings of 11.2%. The lack of benefit with integration of the HVAC system can be attributed to mix of tariffs within the statistics. See Fig. 7 and the subsequent description for more information.

Similar to the critical peak demand savings, the energy cost savings are more significant at the perimeter level. The trend of large incremental savings between the shade Reference and Heuristic-EC cases, and between the Heuristic-EC and MPC-EC cases persists. Depending on the orientation, the incremental median savings between MPC-EC and MPC-EC&HVAC are negligible for the south, west, and north orientations, 1.8, 2.5, and 2.0% respectively, and moderate 4.3% for the east orientation.

3.3. Annual electricity savings

At the whole building level the annual electricity savings for the TOU-high tariff vary between 46.4 MWh for climate zone 8 (Fairbanks, AK – subarctic) and 70.7 MWh for climate zone 3b (Las Vegas, NV – warm dry), see Fig. 2 and Table 7. The median electricity savings for Heuristic-EC are 8.1% or 9.1 kWh/$m^2, for MPC-EC case are 11.4% or 12.9 MWh/$m^2, and for MPC-EC&HVAC case are 10.9% or 12.2 kWh/$m^2. Note that optimizing for minimal energy cost might cause utilization of pre-cooling strategies with the MPC-EC&HVAC case where total electricity demand might increase but demand during the critical periods decreases, see Fig. 7 and subsequent description. The MPC-EC&HVAC control was designed to minimize heating and cooling loads, but since heating energy was supplied by natural gas in the prototype building, it was not included in annual electricity use data.

The electricity savings at the perimeter level are equivalent for the south, west, and east orientations for both the MPC-EC and MPC-EC&HVAC cases, with savings reaching up to 33.4% or 38.9 kWh/$m^2. The savings for the south orientation for Heuristic-EC are equivalent to those for all control cases facing north, with savings reaching up to 27.1% or 27.8 kWh/$m^2. As with the other metrics, the savings at the perimeter level are significantly less than at the building level due to the core to perimeter aspect ratio.

3.4. Emission savings

The emission savings for both, the building and perimeter level follow the same trend as the electricity savings. The savings vary between 4.3 tCO_2 for climate zone 8 (Fairbanks, AK – subarctic) and 7.4 tCO_2 for climate zone 3b (Las Vegas, NV – warm dry), see Fig. 2 and Table 8. Median building level savings are 7.2% for Heuristic-EC, 9.9% for MPC-EC, and 8.0% for MPC-EC&HVAC. Note that similar to electricity savings, the reduction of emissions was not part of the objective of the MPC controller, and techniques such as pre-cooling might increase the overall emissions.

4. Discussion

4.1. Demand response potential and applicability

Historically, DR potential is cost effective for cases where the overall cost of implementing DR is lower than the cost of energy supply, such as peaking generators. In the case of intermittent renewable energy sources, however, the question of how DR should be priced in terms of investment and operational costs is one of the most fundamental questions when evaluating the economic potential of DR options [28]. In a study by Brouwer et al. [29] for example, the investment cost of DR options for a variety of industrial, residential, and tertiary measures were provided as inputs to a larger impact analysis of least cost options for integrating intermittent renewables into low-carbon power systems. The Resource adequacy (RA) metric quantifies how DR contributes to shedding or shifting critical peak demand of the utility's power system, which in turn reduces the amount of generating capacity required to maintain system adequacy. The RA values in Brouwer et al. included

Table 7
Energy savings across five tariffs and sixteen climates.

Orientation	Unit	Heuristic EC			MPC EC			MPC EC & HVAC		
		min	med.	max	min	med.	max	min	med.	max
South	%	13.7	16.3	18.6	27.8	31.7	34.0	25.5	30.3	33.4
	kWh/m^2	14.5	17.6	20.6	26.9	34.4	39.1	24.7	33.0	38.9
West	%	21.1	25.3	27.0	25.1	30.8	33.0	23.2	29.3	32.6
	kWh/m^2	19.6	26.6	30.9	23.3	32.5	38.1	21.5	30.8	37.8
East	%	22.4	24.7	26.8	25.2	30.1	33.2	24.7	28.8	32.6
	kWh/m^2	21.5	25.9	31.3	23.9	32.0	38.8	23.8	30.8	38.4
North	%	18.6	21.3	22.2	22.5	26.2	27.1	20.6	24.7	26.6
	kWh/m^2	16.6	20.5	23.1	20.1	25.3	27.8	18.4	23.8	27.5
Building	%	6.7	8.1	8.6	9.2	11.4	12.3	8.4	10.9	12.3
	kWh/m^2	7.1	9.1	9.9	9.7	12.9	14.2	9.0	12.2	14.2

Table 8
Emission savings across five tariffs and sixteen climates.

Orientation	Unit	Heuristic EC			MPC EC			MPC EC & HVAC		
		min	med.	max	min	med.	max	min	med.	max
South	%	10.0	14.0	16.2	19.9	26.5	28.9	15.0	22.0	28.0
	$kgCO_2/m^2$	1.4	2.1	2.5	2.8	4.0	4.6	2.1	3.3	4.5
West	%	16.6	22.5	25.0	19.4	26.9	29.9	14.1	22.0	28.8
	$kgCO_2/m^2$	2.4	3.4	4.1	2.8	4.0	4.9	2.1	3.3	4.8
East	%	16.9	20.8	23.0	16.7	25.1	28.1	14.7	21.0	27.0
	$kgCO_2/m^2$	2.3	3.0	3.7	2.2	3.6	4.5	2.1	3.0	4.4
North	%	13.8	17.4	18.8	16.7	21.4	22.8	11.0	16.5	21.4
	$kgCO_2/m^2$	2.0	2.3	2.8	2.4	2.9	3.3	1.6	2.3	3.2
Building	%	5.4	7.2	7.8	7.3	9.9	10.7	5.3	8.0	10.4
	$kgCO_2/m^2$	0.8	1.1	1.2	1.1	1.5	1.7	0.8	1.2	1.6

43 $/kW for a 2 h shift in freezer/refrigerator load by switching off the appliance or 100 $/kW for a 6 h delay in use of washing machines and dryers (assuming a 1.0 Euro to U.S. dollar conversion rate). Attitudinal, societal, and other market factors were then used to determine achievable DR potentials. Satchwell et al. [30] used hourly net load savings and hourly marginal system costs for energy, generation capacity, ancillary services, and transmission capacity to disaggregate the economic benefits of energy efficiency (EE) and demand flexibility (DF) on a regional basis throughout the U.S. The data were used to define a national roadmap for grid interactive efficient building technologies. HVAC and envelope EE and DF measures were identified as the single largest drivers of impact estimates and provided the largest aggregate energy and peak demand savings of all analyzed end uses because net demand savings from these measures occurred during critical peak demand periods. Envelope measures included dynamic windows and operable window attachments, such as shades.

The scope of this study did not include the complexity of the Brouwer or Satchwell analysis methods. Instead, RA was calculated using methods described by Alstone et al. (Table G-36) in [31] where, for example, DR-enabled dimmable lighting controls were estimated to have RA values of 438 to 1,239 $/kW for small and large offices. EC windows are estimated to have an incremental cost of 400 $/m^2-window compared to the reference window (dual-pane, spectrally-selective, low-emittance). With increased maturation of the market and introduction of cost-competitive, solution-based EC windows [8], costs are projected to decrease to 100 $/m^2-window. Advances in wireless networking and communications, as well as battery and/or photovoltaic (PV) energy supply to EC windows and motorized shading attachments, are also anticipated to drive installation costs down, opening the opportunity for broader adoption of dynamic window technologies in both new and retrofit construction. Co-benefits reduce the capital cost of a technology for DR by a defined fraction since many advanced technologies are installed for reasons other than DR. In the case of lighting controls, for example, Alstone et al. estimated the fraction of co-benefits to be 75% since this technology is installed largely for energy efficiency. Co-benefits for dynamic windows (discussed below) include reduced energy cost, increased energy efficiency, view, visual and thermal comfort, and reduced HVAC capacity.

- For the median whole building annual critical peak demand reduction of 24.3 kW (TOU-high, 16 climate zones) with an incremental cost of 400 or 100 $/m^2-window, the RA credit for the MPC-EC&HVAC system is 1,302 or 326 $/kW, respectively, assuming 90% co-benefits, or 43.4 or 10.9 $/kW per year over the 30 year estimated life of the window.
- If the customer has already committed to use of dynamic windows with automated control for other reasons, then the added cost for MPC versus heuristic control is estimated to be 10 $/m^2-window for additional MPC software and sensor requirements. The incremental median demand reduction is 10.1 kW. With 50% co-benefits for increased energy efficiency, the RA credit is 392 $/kW or $ 3,960 total. If the cost is defrayed over the 30-year life of the installation, then the RA credit is 13.1 $/kW or $ 132 per year over 30 years.

Note, these RA values are specific to the prototypical medium commercial office building and reflect operational RA, not including long term structural changes to the grid. Also note that we were unable to isolate EC window shed and shift demand reductions based on energy efficiency and demand flexibility from those due to HVAC control because of the integrated systems MPC approach used for determining control states.

Critical peak demand savings were evenly distributed across the three control scenarios, see Fig. 7, with median savings of 9.1, 9.9, and 4.2 kW per building, respectively for the Heuristic-EC, MPC-EC, and MPC-EC&HVAC cases and TOU-high tariff. The TOU tariffs had time-dependent rates where, depending on the time of day, demand rates increased significantly with the intention of triggering local DR control of distributed resources to reduce global stress on the electric power grid. The flat tariffs also included a demand charge which, while lower than the TOU rates, still served to shape demand responsive control. The first sharp reduction in critical peak demand compared to the reference case was due to use of the Heuristic-EC technology where variable solar-optical control offset lighting and cooling loads. Further reduction was achieved with MPC-EC where solar gain and daylight tradeoffs were made on a timestep basis. With MPC-EC&HVAC control, demand savings increased incrementally with the addition of controllable thermal storage via pre-conditioning of the floor. While most MPC-EC&HVAC cases utilized pre-conditioning of the space to shift demand from peak periods, and therefore reducing critical peak demand, the Flat-high tariff did not lead to pre-cooling. However, even without pre-cooling the peak demand during the off-peak and mid-peak periods was reduced significantly, by utilizing smart thermostat control to avoid morning peaks. Note that reduction of morning peaks, especially after the weekend with wider temperature bounds (i.e., Monday mornings) had a significant contribution to the off-peak and mid-peak savings. As demonstrated in the modeled example in Section 3.1, MPC-EC&HVAC control provided an additional advantage in that it was able to adapt to tariff changes. The critical peak of the electric power grid varies in time and magnitude based on local mix of buildings and customer types, and level of DER adoption. In California, for example, PV has a large market share which has led to fast ramping demand in the evening hours, when PV generation decreases to zero during sunset. MPC can continue to minimize peak demand over this transitional period of the electric power grid.

Ensuring resilience of buildings to fluctuations in energy supply during periods of extreme weather events or power outages is another aspect of a low-carbon future [32]. With MPC forecasting, integrated control of solar gains could serve to pre-condition the building in anticipation of the event, enabling comfortable conditions to extend potentially for a longer period after a power outage (i.e., passive survivability [33]). Some EC windows require a small amount of standby power to maintain the windows in a tinted state. If self-powered via photovoltaics and battery storage, the EC windows or motorized shades could enable continued solar control. Such logic for scarcity events could be incorporated in the MPC controller. Note that resilience and DR flexibility objectives may not necessarily be aligned since more stringent solar control could decrease DR lighting energy savings. Additional analysis is needed to determine the extent to which the two objectives differ. For forecasted weather events or planned outages, alternate logic for resilience could be included with DR control.

The end goal of transitioning to renewable energy sources is to reduce GHG emissions. As stated previously, this study's control objective was to minimize energy cost, not GHG emissions, with the assumption that the electricity tariff structure reflected time-dependent clean energy supply and would therefore shape the building's load profile accordingly. Resultant median whole building carbon emission reductions were 7.2 to 9.9%. As a precursor to potential findings had we explicitly modeled the controls to minimize GHG emissions, we look to outcomes from other studies. Zhang et al. [34] found that controls designed to respond to both variable marginal emission factors (MEF) and electricity price resulted in either increased carbon emissions or electricity cost of a campus building cluster, depending on the correlation between price and MEF. In the face of climate-induced extreme events, Levin et al. [35] argues that price signals alone are insufficient to drive improvements in power system resiliency: enhanced reliability metrics are needed to drive investments towards more equitable power solutions, particularly for vulnerable populations that can be disproportionately affected by power outages. Determining whether controls should be focused primarily on GHG emissions and societal impacts instead of financial impacts is clearly a topic of continuing discussion. Assessing the impacts of such control requires further in-depth investigation. Coordination of DR analyses with life cycle GHG emission assessments (material and operating GHG emissions) will be an area of investigation in the newly initiated International Energy Agency Solar Heating and Cooling Program[4] Task 70.

4.2. Co-benefits

Co-benefits are not included in the RA calculation and are used to justify the remaining cost of the installation, i.e., 90%, not addressed by possible DR utility incentives. The co-benefits of the dynamic windows are multi-fold and in part qualitative, which makes them difficult to assess thoroughly. As shown in the Results section, energy use and operating cost decreases significantly with dynamic windows and integrated controls. For all MPC control strategies, even those that involved nighttime pre-cooling of the building's thermal mass, annual electricity use was lower than that of the Reference and Heuristic-EC cases. Additional reductions in HVAC capital and operating costs, i.e., increased efficiency and reduced capacity of central chiller and heating systems, ancillary systems, and air distribution system, are available for deep retrofits and new construction. For DR control with pre-cooling, cost savings due to free cooling in climate zones with low nighttime temperatures were not evaluated.

Traditional DR strategies such as reducing the lighting setpoint or increasing the temperature setpoint range enable load shed to occur irrespective of time of day, weather, or building condition. Such control can negatively affect work performance, i.e., visual performance, occupant comfort, and indoor environmental quality. In the modeled cases, however, the dynamic windows reduced demand by modulating solar heat gain and daylight admission without negative effects. With the MPC-EC&HVAC case, the control supported greater energy efficiency when there was value to do so, and it enabled pre-cooling or pre-heating while maintaining indoor temperatures within the conventional deadband range. Thermal comfort requirements were met for all occupied hours. Visual comfort requirements were met as well. Discomfort glare from the window remained within *imperceptible* levels, i.e., eDGPs $\leq$ 0.34, for 86% of all test cases, and within *noticeable* levels, i.e., eDGPs $\leq$ 0.38, for the remaining 14% of all test cases. Spatial daylight autonomy (sDA), which is an indoor environmental quality metric, met the U.S. Green Building Council's LEED[5] requirements, i.e., a minimum of 50% of the standard workday from 8:00 to 18:00 must achieve 300 lx for 50% of the perimeter zone floor area. The $sDA_{300,50\%}$ levels were between 50% (climate zone 8, Fairbanks, AK – subarctic) and 56.7% (climate zone 7, Duluth, MN – very cold) of the workday period for the DR control cases across all climates and non-north orientations. The three-zone EC window design enabled spatial control of direct sunlight and daylight. Comparable dynamic window designs would need to provide similar independent control of these two variables.

This study did not model controls to accommodate circadian entrainment and other non-visual requirements for daylight but the added energy cost for meeting DA and non-visual requirements with daylight are anticipated to be minor if small incremental increases in daylight transmission occur during late morning to mid-day periods when solar renewable energy is in plentiful supply or when cooling penalties are low, such as during the swing seasons.

With the EC window, transparent views to the outdoors were also maintained. The effects of temporal variations in spectral content due to EC windows on glare perception and non-visual performance are only

[4] IEA Task 70: https://task70.iea-shc.org.
[5] LEED Rating System: https://www.usgbc.org/leed.

starting to be understood [36] and [37] and were not considered in this study.

4.3. Applications

The dynamic solar-optical properties of the EC window spanned a center-of-glass solar heat gain coefficient (SHGC) of 42 to 10% and normal-hemispherical visible transmittance (Tvis) of 60 to 1% with assumed fast switching speeds irrespective of incident solar radiation and outdoor temperatures (i.e., it achieves the targeted state value within five minutes of switching to tint). To reduce occupant disturbance, a derivative penalty can be used to dampen large changes in tint state. Outdoor-mounted, motorized shades such as dual-zone louvered blinds, awnings, or roller shades may provide similar levels of demand savings but may be subject to greater restrictions on movement per time step. There is a good deal of innovation associated with dynamic facade technologies spanning a wide range in cost, architectural aesthetics, and maintenance and operational requirements (e.g., [38], [39], [40], [41], and [42]). Further study is required to determine how best to leverage the unique thermal, solar-optical, ventilative, photovoltaic, and daylighting properties of these systems. A broader array of control strategies should also be considered. For example, shading attachments could accelerate nighttime pre-cooling of thermal mass by enabling radiative exchange with the nighttime sky when automatically raised or retracted. Natural ventilation using operable windows provides additional opportunities for load shed and thermal energy storage.

In terms of applications related to this study, critical peak demand savings were greater for perimeter zones with greater solar exposure. Commercial buildings with large windows and high solar exposure are more likely to realize significant DR savings. These might include small office buildings with single-sided, south-facing windows, floor plate designs with significant perimeter zone exposures, or other building types with internal loads and daytime schedules similar to those of the modeled medium office building.

4.4. Limitations

Characterization of energy flexibility for this type of integrated system is dependent on the specific context, i.e., site, climate, building design, control objectives, user defined needs, tariffs, regional adoption of renewable energy, etc. Standard methods and key performance indices for such characterizations are a subject of general discussion [43]. The U.S. Department of Energy (DOE) has defined prototypical buildings for detailed bottom-up evaluations of emerging technologies and the method in this study used these standard building characteristics to the extent possible. Known limitations when using these prototypical models include the lack of chiller plant models, i.e., cooling loads are converted to electricity with a static COP, and dated building construction and technology parameters that reflect the varied adoption rate of energy-efficiency standards across the nation. For example, the latest *new construction* prototypes use a lighting power density (LPD) of 1 W/ft^2 whereas the latest American Society of Heating, Refrigerating and Air-Conditioning Engineers (ASHRAE) Standard 90.1 mandates 0.62 W/ft^2. The authors acknowledge that improvements in component technologies, for example lower LPD, will affect the results of this study, but DOE has carefully selected these models to provide representative samples and allow equitable comparisons across a broad range of technologies. In addition, the adoption of ASHRAE standards is coupled to the slow moving pace of building development and its time lags.[6] In order to assess the impact of the static COP on the results of this study, an error analysis was conducted for climate zone 2a (Houston, TX – hot humid) and is shown in the Supplementary Materials section S.7. The analysis showed greater benefits when using dynamic versus static COP. For integrated HVAC control strategies, where precooling is typically performed at night when chillers are more efficient due to cooler outdoor air temperatures, the daytime cooling demand is reduced, where chillers are less efficient during the hotter daytime temperatures, leading to additional savings in comparison with the static COP. The summer peak demand was reduced by an additional 5.3% and annual electricity cost was reduced by another 2.6% when modeling dynamic chiller plant performance. However, the vast varieties of cooling supply, plant operation, and optimization are out of scope of this study, hence the use of the static COP to generalize results. But given the results of the error analysis, the savings potential presented in this paper can be seen as an conservative estimate. Future studies may include more detailed HVAC and chiller plant models to capitalize those additional benefits.

In terms of practical feasibility, configuring and calibrating grey box resistance-capacitance thermal models are a well known challenge with MPC. Model inaccuracy can degrade controller performance significantly from optimal. In this study, the RC model was tuned based on feedback from environmental conditions where solar loads were well characterized due to explicit knowledge of the state of the window system. For other types of DR controllers that do not involve dynamic facades, real-time information on interior solar and daylight loads are not available. Blum et al. [44] determined that noisy solar data (i.e., direct transmitted solar radiation on interior mass) had a significant effect on model inaccuracy whereas outdoor dry bulb temperature (i.e., conductive loads) had a lesser effect. Other areas of mismatch between the MPC controller and simulated building were the position of the occupant (i.e., MPC assumed worst-case facing due south whereas simulation modeled parallel to window, see Table 3) and heating system (i.e., MPC assumed fixed efficiency electric heating whereas simulation modeled natural gas fired system). In [45], black box models for indoor air temperature and indoor illuminance were trained using data from a virtual EnergyPlus building to demonstrate how MPC-based control of shading, lighting, and HVAC could be implemented at lower cost and scale. In [46], a hybrid MPC approach involving machine learning techniques was used to control a blind to minimize thermal discomfort and maintain a minimal level of daylight illuminance. An exploratory study of dynamic facades and HVAC control using data-driven artificial neural networks with reinforcement learning was also conducted [47].

Further work in this area may improve performance of HVAC controls as well as integrated systems controls. There is considerable effort underway to build the simulation tools needed to develop and evaluate demand flexible controls at individual building and community scales. The workflow mechanics between Radiance and EnergyPlus within Spawn [48] are being streamlined and scheduled to complete within the next year.

5. Conclusion

Modeled results for a prototypical new medium office building indicate that dynamic windows have significant potential to support demand side flexibility and reliability of the electricity grid, which is becoming increasingly reliant on intermittent renewable energy sources. Estimated whole building annual critical peak demand reductions range between 14.6 kW (Boulder, CO – cool dry) to 27.8 kW (Albuquerque, NM – mixed dry) with a median of 24.3 kW (4.4 W/m^2) across 16 U.S. climate zones for the most stringent time-of-use tariff, and occur largely irrespective of cloudy or sunny solar conditions, supporting grid flexibility even when there is moderate stress on the grid. The median resource adequacy cost ranges between 13.1 to 43.4 $/kW per year for the dynamic window and model predictive control technology, which is cost competitive to existing technologies (e.g., demand response enabled dimmable lighting) and is therefore of sufficient magnitude to warrant serious consideration for inclusion in demand response portfolios.

[6] At present, about 50% of the states in the U.S. have adopted the ASHRAE 90.1-2013 code which mandates an LPD of no greater than 1.0 W/ft^2 and about 25% have adopted the 90.1-2016 code with a mandated LPD of 0.8 W/ft^2.

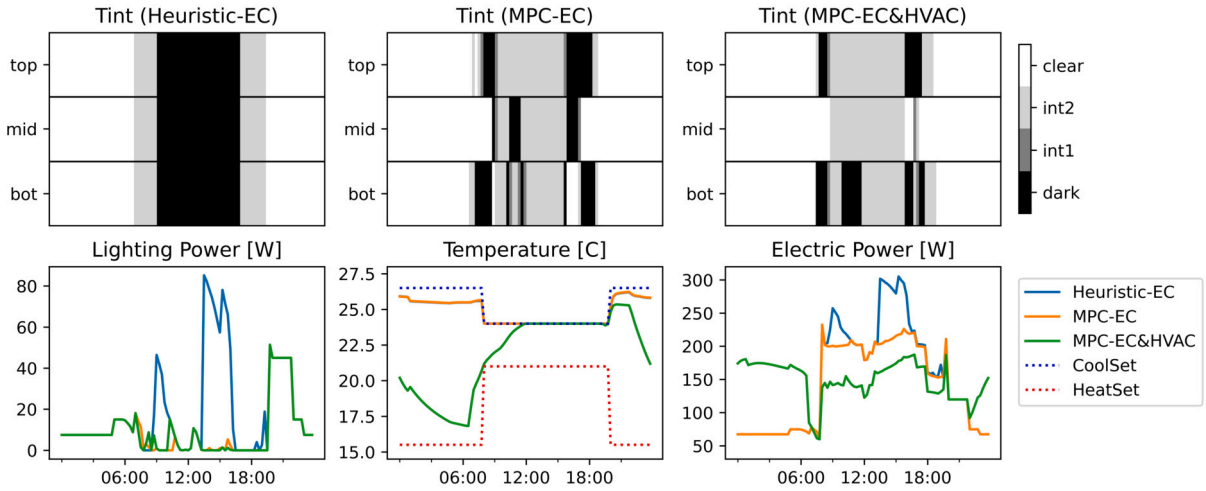

Fig. A-1. Controller operation for one day of a facade with three horizontal electrochromic window zones, each with four tint states: clear (white), Intermediate 1 (light gray), Intermediate 2 (dark gray), and dark (black). Solar heat gain coefficient range: 0.42 (clear), 0.16, 0.12, 0.10 (dark). Visible transmittance range: 0.60 (clear), 0.18, 0.06, 0.01 (dark). South-facing perimeter office, climate zone 3bc (Los Angeles, CA – warm marine), TOU-high. Top: Tint patterns for the three zones (top, middle, bottom) and across three control cases (left: manufacturer typical heuristic control, middle: control with MPC of electrochromic windows only, right: control with MPC of integrated electrochromic and HVAC systems). Bottom-left: Resulting power consumption of the lighting system across the three control cases. Bottom-middle: Resulting room air temperatures and thermostat setpoints for heating and cooling. Bottom-right: Resulting total electricity consumption including plug-loads, HVAC, and lighting.

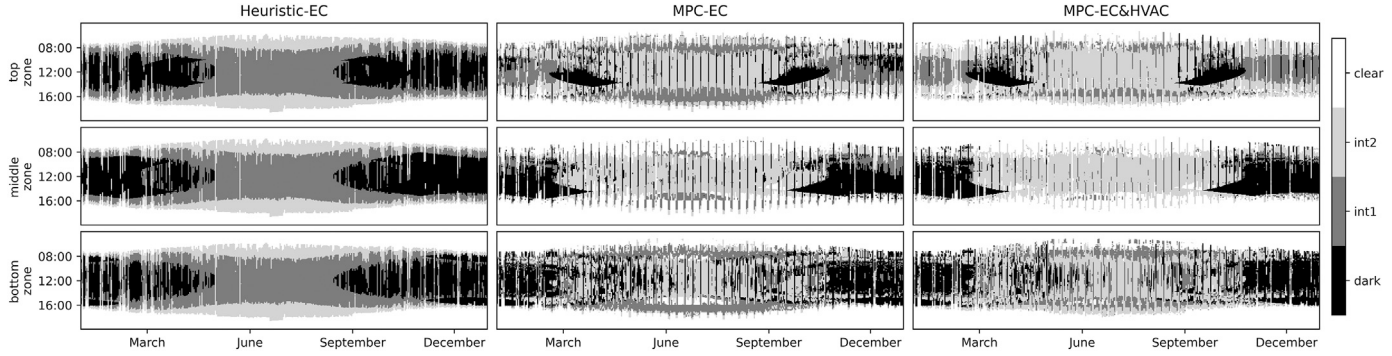

Fig. A-2. Annual tint pattern for a facade with three horizontal electrochromic window zones, each with four tint states: clear (white), Intermediate 1 (light gray), Intermediate 2 (dark gray), and dark (black). Solar heat gain coefficient range: 0.42 (clear), 0.16, 0.12, 0.10 (dark). Visible transmittance range: 0.60 (clear), 0.18, 0.06, 0.01 (dark). South-facing perimeter office, climate zone 3bc (Los Angeles, CA – warm marine), TOU-high. Left: Manufacturer typical heuristic control. Middle: Control with MPC of electrochromic windows only. Right: Control with MPC of integrated electrochromic and HVAC systems.

Declaration of competing interest

The authors declare that they have no known competing financial interests or personal relationships that could have appeared to influence the work reported in this paper.

Data availability

Data will be made available on request.

Acknowledgement

This work was supported by the Assistant Secretary for Energy Efficiency and Renewable Energy, Building Technologies Office of the U.S. Department of Energy under Contract No. DE-AC02-05CH11231. Additional support was provided by the California Energy Commission under the Electric Program Investment Charge (EPIC) Program, Solicitation Number EPC-14-066, that was awarded to Lawrence Berkeley National Laboratory for the work herein.

Appendix A

See Figs. A-1, A-2 and Table A-1.

Appendix B. Supplementary material

Supplementary material related to this article can be found online at https://doi.org/10.1016/j.enbuild.2023.113481.

Table A-1
Whole building annual results for cases Reference (Ref.), Heuristic-EC (Heur.), MPC-EC (MPC1), and MPC-EC&HVAC (MPC2) across all 16 U.S. climate zones and five tariffs.

Climate	Case	Peak Demand [kW]					Energy Cost [k$]					Electricity Demand [MWh]					Emissions [tCO_2]				
		Flat high	Tou high	Flat low	Tou low	Tou late	Flat high	Tou high	Flat low	Tou low	Tou late	Flat high	Tou high	Flat low	Tou low	Tou late	Flat high	Tou high	Flat low	Tou low	Tou late
1a	Ref.	138.2	138.2	138.2	138.2	138.2	49.5	72.0	19.7	22.6	42.5	576.2	576.2	576.2	576.2	576.2	77.9	77.9	77.9	77.9	77.9
	Heur.	128.7	128.7	128.7	128.7	128.7	45.5	66.2	18.1	20.8	39.1	529.4	529.4	529.4	529.4	529.4	72.2	72.2	72.2	72.2	72.2
	MPC1	118.8	118.9	118.8	118.8	118.8	43.9	63.7	17.5	20.0	37.8	510.8	511.3	510.8	510.8	510.8	70.1	70.2	70.1	70.1	70.1
	MPC2	118.5	114.4	118.2	115.4	118.7	44.0	63.5	17.5	19.7	38.0	511.3	515.3	512.6	516.3	513.3	70.3	71.8	71.0	72.4	71.3
2a	Ref.	140.8	140.8	140.8	140.8	140.8	48.6	70.8	19.3	22.3	41.7	565.1	565.1	565.1	565.1	565.1	76.5	76.5	76.5	76.5	76.5
	Heur.	131.0	131.0	131.0	131.0	131.0	44.7	65.1	17.7	20.4	38.5	519.5	519.5	519.5	519.5	519.5	71.0	71.0	71.0	71.0	71.0
	MPC1	119.2	119.3	119.2	119.2	119.2	43.1	62.6	17.1	19.6	37.2	501.0	501.4	501.0	501.0	501.0	68.9	69.0	68.9	68.9	68.9
	MPC2	118.9	113.8	118.0	114.5	117.8	43.1	62.4	17.2	19.4	37.3	501.6	506.1	503.4	506.9	504.1	69.2	70.8	70.0	71.1	70.4
2b	Ref.	143.1	143.1	143.1	143.1	143.1	50.2	73.1	20.0	23.0	43.2	584.3	584.3	584.3	584.3	584.3	79.3	79.3	79.3	79.3	79.3
	Heur.	134.0	134.0	134.0	134.0	134.0	46.0	67.0	18.3	21.0	39.6	534.9	534.9	534.9	534.9	534.9	73.1	73.1	73.1	73.1	73.1
	MPC1	124.0	123.9	123.9	124.0	124.0	44.2	64.1	17.5	20.1	38.1	513.8	514.1	513.8	513.8	513.8	70.8	70.9	70.8	70.8	70.8
	MPC2	123.8	117.3	121.3	120.5	121.8	44.2	63.9	17.6	19.8	38.3	514.4	518.8	516.3	518.9	516.9	71.1	72.7	72.1	72.9	72.3
3a	Ref.	137.8	137.8	137.8	137.8	137.8	47.9	69.8	19.0	22.0	41.2	556.9	556.9	556.9	556.9	556.9	75.4	75.4	75.4	75.4	75.4
	Heur.	129.3	129.3	129.3	129.3	129.3	43.9	64.0	17.4	20.1	37.8	510.7	510.7	510.7	510.7	510.7	69.8	69.8	69.8	69.8	69.8
	MPC1	119.2	119.2	119.2	119.2	119.2	42.4	61.6	16.8	19.3	36.6	493.0	493.4	493.0	493.0	493.0	67.9	68.0	67.9	67.9	67.9
	MPC2	119.0	113.0	116.5	114.4	117.2	42.5	61.5	16.9	19.1	36.8	494.1	498.1	495.6	498.8	496.1	68.3	69.7	68.9	70.0	69.3
3b	Ref.	142.6	142.6	142.6	142.6	142.6	49.5	72.1	19.7	22.6	42.5	575.6	575.6	575.6	575.6	575.6	78.0	78.0	78.0	78.0	78.0
	Heur.	133.2	133.2	133.2	133.2	133.2	45.2	66.0	18.0	20.7	39.0	526.1	526.1	526.1	526.1	526.1	72.1	72.1	72.1	72.1	72.1
	MPC1	123.3	123.1	123.2	123.2	123.2	43.4	63.1	17.2	19.8	37.5	504.9	505.3	504.8	504.8	504.8	69.8	69.8	69.8	69.8	69.8
	MPC2	123.0	116.9	120.6	119.1	120.0	43.5	63.0	17.3	19.6	37.7	505.6	504.8	507.6	509.7	507.8	70.0	70.6	70.9	71.6	71.2
3bc	Ref.	137.5	137.5	137.5	137.5	137.5	47.9	69.8	19.0	22.0	41.1	557.1	557.1	557.1	557.1	557.1	75.2	75.2	75.2	75.2	75.2
	Heur.	127.7	127.7	127.7	127.7	127.7	44.0	64.0	17.5	20.2	37.8	511.4	511.4	511.4	511.4	511.4	69.7	69.7	69.7	69.7	69.7
	MPC1	117.3	117.6	117.3	117.3	117.3	42.3	61.5	16.8	19.3	36.5	492.3	492.8	492.3	492.3	492.3	67.7	67.7	67.7	67.7	67.7
	MPC2	117.0	110.4	114.5	112.7	117.0	42.4	61.4	16.9	19.1	36.7	493.2	498.3	495.5	498.6	495.3	68.0	69.7	68.9	69.9	69.0
3c	Ref.	136.0	136.0	136.0	136.0	136.0	47.2	68.9	18.8	21.7	40.5	549.1	549.1	549.1	549.1	549.1	74.1	74.1	74.1	74.1	74.1
	Heur.	125.8	125.8	125.8	125.8	125.8	43.3	63.1	17.2	19.9	37.3	503.8	503.8	503.8	503.8	503.8	68.8	68.8	68.8	68.8	68.8
	MPC1	114.7	114.6	114.5	114.5	114.7	41.7	60.5	16.6	19.0	35.9	484.7	485.1	484.7	484.7	484.7	66.7	66.7	66.7	66.7	66.7
	MPC2	114.5	113.4	113.9	112.1	114.4	41.8	60.6	16.6	18.8	36.1	485.6	490.1	487.0	490.8	486.5	67.0	68.4	67.5	68.7	67.4
4a	Ref.	137.7	137.7	137.7	137.7	137.7	47.1	68.8	18.7	21.6	40.5	548.1	548.1	548.1	548.1	548.1	74.4	74.4	74.4	74.4	74.4
	Heur.	129.1	129.1	129.1	129.1	129.1	43.3	63.1	17.2	19.8	37.3	503.6	503.6	503.6	503.6	503.6	69.2	69.2	69.2	69.2	69.2
	MPC1	122.4	122.6	122.4	122.4	122.4	41.8	60.7	16.6	19.0	36.1	485.8	486.1	485.8	485.8	485.8	67.3	67.3	67.3	67.3	67.3
	MPC2	122.1	120.0	121.7	118.5	122.0	41.9	60.6	16.7	18.9	36.3	487.2	490.6	488.3	491.0	488.9	67.7	68.9	68.2	69.1	68.6
4b	Ref.	140.4	140.4	140.4	140.4	140.4	47.9	69.9	19.0	22.0	41.2	557.0	557.0	557.0	557.0	557.0	75.5	75.5	75.5	75.5	75.5
	Heur.	130.4	130.4	130.4	130.4	130.4	43.8	63.9	17.4	20.0	37.7	509.1	509.1	509.1	509.1	509.1	69.7	69.7	69.7	69.7	69.7
	MPC1	118.8	118.7	118.7	118.7	118.7	42.0	61.1	16.7	19.1	36.3	488.7	489.1	488.7	488.7	488.7	67.5	67.5	67.5	67.5	67.5
	MPC2	118.4	112.6	116.9	114.9	116.7	42.1	61.0	16.8	19.0	36.5	489.9	494.2	491.9	493.9	492.1	67.9	69.4	68.8	69.3	69.0
4c	Ref.	138.2	138.2	138.2	138.2	138.2	46.4	67.8	18.4	21.3	39.9	539.9	539.9	539.9	539.9	539.9	73.2	73.2	73.2	73.2	73.2
	Heur.	130.8	130.8	130.8	130.8	130.8	42.7	62.3	17.0	19.5	36.8	496.9	496.9	496.9	496.9	496.9	68.2	68.2	68.2	68.2	68.2
	MPC1	118.7	118.7	118.7	118.7	118.7	41.5	60.2	16.4	18.8	35.7	482.8	482.2	481.1	481.1	481.1	66.7	66.6	66.4	66.4	66.4
	MPC2	118.3	118.4	118.2	117.9	118.5	41.5	60.1	16.5	18.7	35.9	482.3	486.0	483.8	485.9	483.6	66.8	68.0	67.5	68.1	67.5
5a	Ref.	138.3	138.3	138.3	138.3	138.3	46.4	67.8	18.4	21.3	40.0	540.0	540.0	540.0	540.0	540.0	73.6	73.6	73.6	73.6	73.6
	Heur.	129.0	129.0	129.0	129.0	129.0	42.8	62.4	17.0	19.5	36.9	497.5	497.5	497.5	497.5	497.5	68.8	68.8	68.8	68.8	68.8
	MPC1	118.9	118.9	118.8	118.9	118.9	41.4	60.1	16.4	18.8	35.8	481.1	481.4	481.1	481.1	481.1	67.1	67.1	67.1	67.1	67.1
	MPC2	118.9	114.2	115.9	113.9	116.1	41.5	60.1	16.5	18.7	36.0	482.9	486.1	484.2	485.9	484.2	67.5	68.8	68.2	68.8	68.4

Climate	Case	Peak Demand [kW]				Energy Cost [k$]				Electricity Demand [MWh]				Emissions [tCO_2]			
		Flat high	Tou high	Flat low	Tou late	Flat high	Tou high	Flat low	Tou late	Flat high	Tou high	Flat low	Tou late	Flat high	Tou high	Flat low	Tou late
5b	Ref.	143.7	143.7	143.7	143.7	47.0	68.6	18.7	40.4	546.4	546.4	546.4	546.4	74.2	74.2	74.2	74.2
	Heur.	131.5	131.5	131.5	131.5	43.0	62.8	17.1	37.1	500.5	500.5	500.5	500.5	68.9	68.9	68.9	68.9
	MPC1	132.1	132.1	132.1	132.1	41.4	60.3	16.5	35.8	481.9	482.2	481.9	481.9	66.9	66.9	66.9	66.9
	MPC2	131.8	129.1	131.6	131.9	41.6	60.2	16.6	36.0	483.5	487.2	485.0	484.9	67.3	68.6	68.0	68.2
6a	Ref.	139.4	139.4	139.4	139.4	46.3	67.6	18.4	39.9	538.3	538.3	538.3	538.3	73.8	73.8	73.8	73.8
	Heur.	130.4	130.4	130.4	130.4	42.6	62.1	16.9	36.8	495.9	495.9	495.9	495.9	69.1	69.1	69.1	69.1
	MPC1	120.0	119.9	119.8	119.9	41.2	59.9	16.4	35.6	479.2	479.4	479.2	479.2	67.3	67.3	67.3	67.3
	MPC2	119.8	113.6	114.8	115.3	41.4	59.8	16.5	35.8	481.0	483.9	482.4	484.0	67.7	68.9	68.5	69.0	68.4
6b	Ref.	139.3	139.3	139.3	139.3	46.2	67.5	18.4	39.8	537.7	537.7	537.7	537.7	73.4	73.4	73.4	73.4	73.4
	Heur.	131.3	131.3	131.3	131.3	42.6	62.1	16.9	36.7	495.2	495.2	495.2	495.2	68.5	68.5	68.5	68.5	68.5
	MPC1	118.1	118.1	118.1	118.1	41.1	59.7	16.3	35.5	477.6	477.8	477.6	477.6	66.6	66.6	66.6	66.6	66.6
	MPC2	118.1	114.7	117.1	114.7	41.2	59.6	16.4	35.7	479.4	480.9	480.9	480.7	67.0	67.9	67.8	68.3	67.8
7	Ref.	135.8	135.8	135.8	135.8	45.6	66.6	18.1	39.3	530.0	530.0	530.0	530.0	73.1	73.1	73.1	73.1	73.1
	Heur.	131.1	131.1	131.1	131.1	42.1	61.3	16.7	36.3	489.5	489.5	489.5	489.5	68.9	68.9	68.9	68.9	68.9
	MPC1	120.6	118.5	118.5	120.6	40.9	59.1	16.2	35.3	475.1	473.5	473.2	475.1	67.4	67.1	67.1	67.1	67.4
	MPC2	118.4	114.6	114.9	113.7	40.9	59.1	16.3	35.3	475.1	477.4	476.1	475.4	67.4	68.4	68.0	68.6	67.9
8	Ref.	138.0	138.0	138.0	138.0	45.5	66.5	18.1	39.2	529.7	529.7	529.7	529.7	75.0	75.0	75.0	75.0	75.0
	Heur.	128.4	128.4	128.4	128.4	42.5	61.8	16.9	36.6	494.2	494.2	494.2	494.2	70.9	70.9	70.9	70.9	70.9
	MPC1	118.9	118.9	118.9	118.9	41.4	60.0	16.4	35.6	481.0	481.2	481.0	481.0	69.5	69.5	69.5	69.5	69.5
	MPC2	118.9	119.4	119.2	119.0	41.5	60.0	16.5	35.7	482.4	483.3	483.8	485.0	69.7	70.6	70.6	71.0	70.4

References

[1] B.V. Mathiesen, H. Lund, K. Karlsson, 100% renewable energy systems, climate mitigation and economic growth, Appl. Energy 88 (2) (2011) 488–501.

[2] U.S. Energy Information Administration, Annual energy outlook 2020 with projections to 2050 [Online], Available: https://www.eia.gov/outlooks/aeo/pdf/AEO2020%20Full%20Report.pdf, 2020.

[3] M. Neukomm, V. Nubbe, R. Fares, Grid-Interactive Efficient Buildings Technical Report Series: Overview of Research Challenges and Gaps, National Renewable Energy Laboratory, Golden, CO (United States), 2019.

[4] C. Harris, S. Mumme, M. LaFrance, M. Neukomm, K. Sawyer, Grid-Interactive Efficient Buildings Technical Report Series: Windows and Opaque Envelope, National Renewable Energy Laboratory, Golden, CO (United States), 2019.

[5] M. Sofos, J.T. Langevin, M. Deru, E. Gupta, K.S. Benne, D. Blum, T. Bohn, R. Fares, N. Fernandez, G. Fink, et al., Innovations in Sensors and Controls for Building Energy Management: Research and Development Opportunities Report for Emerging Technologies, National Renewable Energy Laboratory, Golden, CO (United States), 2020.

[6] M. Rakibuddin, M.A. Shinde, H. Kim, Facile sol–gel fabrication of MoS_2 bulk, flake and quantum dot for electrochromic device and their enhanced performance with WO_3, Electrochim. Acta (2020) 136403.

[7] A. Llordés, Y. Wang, A. Fernandez-Martinez, P. Xiao, T. Lee, A. Poulain, O. Zandi, C.A.S. Cabezas, G. Henkelman, D.J. Milliron, Linear topology in amorphous metal oxide electrochromic networks obtained via low-temperature solution processing, Nat. Mater. 15 (12) (2016) 1267–1273.

[8] K. Tang, K. Dong, J. i, M. Gordon, F. Reichertz, H. Kim, Y. Rho, Q. Wang, C. Lin, C. Grigoropoulos, et al., Temperature-adaptive radiative coating for all-season household thermal regulation, Science 372 (2) (2021) 1504–1509.

[9] L.L. Fernandes, E.S. Lee, A. McNeil, J.C. Jonsson, T. Nouidui, X. Pang, S. Hoffmann, Angular selective window systems: assessment of technical potential for energy savings, Energy Build. 90 (2015) 188–206.

[10] D. Gyalistras, M. Gwerder, F. Oldewurtle, C. Jones, M. Morari, Analysis of energy savings potentials for integrated room automation, in: Proceedings of the Clima, RHEVA World Congress, Antalya, Turkey, 2010.

[11] K. Klein, S. Herkel, H.-M. Henning, C. Felsmann, Load shifting using the heating and cooling system of an office building: quantitative potential evaluation for different flexibility and storage options, Appl. Energy 203 (2017) 917–937.

[12] M. Liu, P. Heiselberg, Energy flexibility of a nearly zero-energy building with weather predictive control on a convective building energy system and evaluated with different metrics, Appl. Energy 233 (2019) 764–775.

[13] C.D. Korkas, S. Baldi, I. Michailidis, E.B. Kosmatopoulos, Occupancy-based demand response and thermal comfort optimization in microgrids with renewable energy sources and energy storage, Appl. Energy 163 (2016) 93–104.

[14] K.-h. Lee, J.E. Braun, Model-based demand-limiting control of building thermal mass, Build. Environ. 43 (10) (2008) 1633–1646.

[15] J. Cai, J.E. Braun, Assessments of demand response potential in small commercial buildings across the United States, Sci. Technol. Built Environ. 25 (10) (2019) 1437–1455.

[16] B. Coffey, A. McNeil, T. Nouidui, E. Lee, Automated production of optimization-based control logics for dynamic façade systems, with experimental application to two-zone external venetian blinds, CEC PIER Technical Report, 2013 [Online], Available: https://eta-publications.lbl.gov/publications/automated-production-optimization.

[17] C. Gehbauer, D.H. Blum, T. Wang, E.S. Lee, An assessment of the load modifying potential of model predictive controlled dynamic facades within the California context, Energy Build. 210 (2020) 109762.

[18] C. Gehbauer, Distributed optimal and predictive energy resources (DOPER), in: Lawrence Berkeley National Laboratory, Berkeley, CA (United States), 2019 [Online], Available: https://github.com/LBNL-ETA/DOPER.

[19] C.A. Antonopoulos, T.L. Gilbride, E.R. Margiotta, C.E. Kaltreider, Guide to Determining Climate Zone by County: IECC and Building America 2021 Updates, Pacific Northwest National Laboratory, Richland, WA (United States), 2022.

[20] A. McNeil, E.S. Lee, A validation of the radiance three-phase simulation method for modelling annual daylight performance of optically complex fenestration systems, J. Build. Perform. Simul. 6 (1) (2013) 24–37.

[21] J. Wienold, Dynamic daylight glare evaluation, in: Proceedings of Building Simulation, 2009, pp. 944–951.

[22] J. Klems, A New Method for Predicting the Solar Heat Gain of Complex Fenestration Systems: II, Detailed Description of the Matrix Layer Calculation, Lawrence Berkeley National Laboratory, Berkeley, CA (United States), 1993.

[23] E.S. Lee, D. Geisler-Moroder, G. Ward, Modeling the direct sun component in buildings using matrix algebraic approaches: methods and validation, Sol. Energy 160 (2018) 380–395.

[24] M. Deru, K. Field, D. Studer, K. Benne, B. Griffith, P. Torcellini, B. Liu, M. Halverson, D. Winiarski, M. Rosenberg, et al., US Department of Energy Commercial Reference Building Models of the National Building Stock, National Renewable Energy Laboratory, Golden, CO (United States), 2011.

[25] C. Gehbauer, D.H. Blum, T. Wang, E.S. Lee, Integrated Dynamic Facade Control with an Agent-Based Architecture for Commercial Buildings, Lawrence Berkeley National Laboratory, Berkeley, CA (United States), 2020.

[26] P. Gagnon, B. Cowiestoll, M. Schwarz, Cambium 2022 Scenario Descriptions and Documentation, National Renewable Energy Laboratory, Golden, CO (United States), 2022.
[27] U.S. Environmental Protection Agency, Inventory of US Greenhouse Gas Emissions and Sinks: 1990–2020 (epa 430-r-22-003), 2022.
[28] P. Pinson, H. Madsen, Benefits and challenges of electrical demand response: a critical review, Renew. Sustain. Energy Rev. 39 (2014) 686–699.
[29] A. Brouwer, M. van den Broek, W. Zappa, W. Turkenburg, A. Faaij, Least-cost options for integrating intermittent renewables in low-carbon power systems, Appl. Energy 161 (2016) 48–74.
[30] A. Satchwell, M. Piette, A. Khandekar, J. Granderson, N. Frick, R. Hledik, A. Faruqui, L. Lam, S.R.J. Cohen, K. Wang, A National Roadmap for Grid-Interactive Efficient Buildings, Lawrence Berkeley National Laboratory, Berkeley, CA (United States), 2021.
[31] P. Alstone, J. Potter, M.A. Piette, P. Schwartz, M.A. Berger, L.N. Dunn, S.J. Smith, M.D. Sohn, A. Aghajanzadeh, S. Stensson, et al., 2025 California Demand Response Potential Study-Charting California's Demand Response Future. Final Report on Phase 2 Results, Lawrence Berkeley National Laboratory, Berkeley, CA (United States), 2017.
[32] S. Attia, R. Levinson, E. Ndongo, P. Holzer, O.B. Kazanci, S. Homaei, C. Zhang, B.W. Olesen, D. Qi, M. Hamdy, et al., Resilient cooling of buildings to protect against heat waves and power outages: key concepts and definition, Energy Build. 239 (2021) 110869.
[33] R. Li, A.J. Satchwell, D. Finn, T.H. Christensen, M. Kummert, J. Le Dréau, R.A. Lopes, H. Madsen, J. Salom, G. Henze, et al., Ten questions concerning energy flexibility in buildings, Build. Environ. 223 (2022) 109461.
[34] H. Zhang, F. Xiao, C. Zhang, R. Li, A multi-agent system based coordinated multi-objective optimal load scheduling strategy using marginal emission factors for building cluster demand response, Energy Build. 281 (2023) 112765.
[35] T. Levin, A. Botterud, W.N. Mann, J. Kwon, Z. Zhou, Extreme weather and electricity markets: key lessons from the February 2021 Texas crisis, Joule 6 (1) (2022) 1–7.
[36] S. Jain, C. Karmann, J. Wienold, Behind electrochromic glazing: assessing user's perception of glare from the sun in a controlled environment, Energy Build. 256 (2022) 111738.
[37] E.S. Lee, B.S. Matusiak, D. Geisler-Moroder, S.E. Selkowitz, L. Heschong, Advocating for view and daylight in buildings: next steps, Energy Build. 265 (2022) 112079.
[38] F. Isaia, M. Fiorentini, V. Serra, A. Capozzoli, Enhancing energy efficiency and comfort in buildings through model predictive control for dynamic façades with electrochromic glazing, J. Build. Eng. 43 (2021) 102535.
[39] C. Martín-Gómez, A. Zuazua-Ros, K.D.V. de Lersundi, B.S. Saiz-Ezquerra, M. Ibáñez-Puy, Integration development of a ventilated active thermoelectric envelope (VATE): constructive optimization and thermal performance, Energy Build. 231 (2021) 110593.
[40] E.C. Lucchino, F. Goia, Multi-domain model-based control of an adaptive façade based on a flexible double skin system, Energy Build. 285 (2023) 112881.
[41] M. Voigt, D. Roth, H. Binz, Challenges with adaptive facades-a life cycle perspective, in: 16th Advanced Building Skins Conference & Expo, 2021, pp. 459–468.
[42] E. Taveres-Cachat, S. Grynning, J. Thomsen, S. Selkowitz, Responsive building envelope concepts in zero emission neighborhoods and smart cities—a roadmap to implementation, Build. Environ. 149 (2019) 446–457.
[43] S. Jensen, H. Madsen, R. Lopes, R.G. Junker, D. Aelenei, R. Li, S. Metzger, K. Lindberg, A. Marszal, M. Kummert, et al., Energy Flexibility as a Key Asset in a Smart Building Future: Contribution of Annex 67 to the European Smart Building Initiatives, 2017.
[44] D. Blum, K. Arendt, L. Rivalin, M. Piette, M. Wetter, C. Veje, Practical factors of envelope model setup and their effects on the performance of model predictive control for building heating, ventilating, and air conditioning systems, Appl. Energy 236 (2019) 410–425.
[45] M. Knudsen, S. Petersen, Economic model predictive control of space heating and dynamic solar shading, Energy Build. 209 (2020) 109661.
[46] K. Le, R. Bourdais, H. Guéguen, From hybrid model predictive control to logical control for shading system: a support vector machine approach, Energy Build. 84 (2014) 352–359.
[47] C. Gehbauer, A. Rippl, E. Lee, Advanced control of dynamic facades and HVAC with reinforcement learning based on standardized co-simulation, in: Proceedings of the Building Simulation Conference, 2021.
[48] T. Wang, G.J. Ward, E.S. Lee, A Python library for radiance matrix-based simulation control and energyplus integration, in: Proceedings of the Building Simulation Conference, 2022.

References in supplementary material

[49] T.S. Nouidui, M. Wetter, W. Zuo, Validation of the window model of the modelica buildings library, Proc. SimBuild 5 (1) (2012) 529–536.
[50] L.L. Fernandes, E.S. Lee, D. Dickerhoff, A. Thanachareonkit, T. Wang, C. Gehbauer, Electrochromic Window Demonstration at the John E. Moss Federal Building, 650 Capitol Mall, Sacramento, California, Lawrence Berkeley National Laboratory, Berkeley, CA (United States), 2018.
[51] International Code Council, International Energy Conservation Code, 2000.